Temozolomide down-regulates P-glycoprotein expression in glioblastoma stem cells by interfering with the Wnt3a/GSK3/β-catenin pathway

Temozolomide down-regulates P-glycoprotein expression in glioblastoma stem cells by interfering with the Wnt3a/GSK3/β-catenin pathway.

Chiara Riganti, Iris Chiara Salaroglio, Valentina Caldera, Ivana Campia, Joanna Kopecka, Marta Mellai, Laura Annovazzi, Amalia Bosia, Dario Ghigo, Davide Schiffer

Department of Oncology, University of Turin, via Santena 5/bis, 10126, Turin, Italy (C.R., I.C.S., I.C., J.K., A.B., D.G.); Center for Experimental Research and Medical Studies (Ce.R.M.S.), University of Turin, via Santena 5/bis, 10126, Turin, Italy (C.R., A.B., D.G.); Neuro-bio-oncology Center, Policlinico di Monza Foundation, Via Pietro Micca 29, 13100, Vercelli, Italy (V.C., M.M., L.A., D.S.)

Running title: temozolomide decreases Wnt3a and P-glycoprotein

Corresponding author: Chiara Riganti, Department of Oncology, University of Turin, via Santena 5/bis, 10126, Turin, Italy; phone: +39-011-6705857; phone: +39-011-6705857; fax: +39-011-6705845; email: chiara.riganti@unito.it

Funding.

This work has been supported by Compagnia di San Paolo "Programma Neuroscienze", Italian Association for Cancer Research (AIRC), Italian Ministry of University and Research (MIUR).

Conflict of interest.

The authors declare no conflict of interest.

Abstract

Background. Glioblastoma multiforme stem cells display a highly chemoresistant *phenotype, whose molecular basis were poorly known. We aim to clarify this issue and to* investigate the effects of temozolomide on chemoresistant stem cells.

Methods. A panel of human glioblastoma cultures, grown as stem cells (neurospheres) and adherent cells, were used.

Results. Neurospheres had a multidrug resistant phenotype compared with adherent cells. Such chemoresistance was overcome by apparently non-cytotoxic doses of temozolomide, which chemosensitize glioblastoma cells to doxorubicin, vinblastine and etoposide. This effect was selective for P-glycoprotein (Pgp) substrates and for stem cells, leading to investigate whether there was a correlation between the expression of Pgp and the activity of typical stemness pathways. We found that *Wnt3a* and *ABCB1*, which encodes for Pgp, were both highly expressed in glioblastoma stem cells and reduced by temozolomide. Temozolomide-treated cells had increased methylation of the CpG islands in the *Wnt3a* gene promoter, decreased expression of Wnt3a, disrupted glycogen synthase-3 kinase/β-catenin axis, reduced transcriptional activation of *ABCB1*, lower amount and activity of Pgp. Wnt3a overexpression was sufficient to transform adherent cells into neurospheres and to simultaneously increase proliferation and *ABCB1* expression. On the contrary glioblastoma stem cells silenced for Wnt3a lost the ability to form neurospheres and reduced at the same time the proliferation rate and the *ABCB1* levels.

Conclusions. Our work suggests that Wnt3a is an autocrine mediator of stemness, proliferation and chemoresistance in human glioblastoma and that temozolomide may chemosensitize the stem cell population by down-regulating the Wnt3a signaling.

Keywords: glioblastoma stem cells; temozolomide; Wnt3a; ABCB1/P-glycoprotein

Introduction

Glioblastoma multiforme (GBM) is the most malignant and frequent intra-assial tumor of the central nervous system. Despite the improvement of neurosurgery, radiotherapy and chemotherapy, no local control of the disease is today possible [1,2]. The failure of chemotherapy is due to the tumor polyclonality, to its modalities of invasion and to the resistance to therapies. The presence of the so-called cancer stem cells (CSCs) within GBM has been suggested as another possible reason of chemoresistance [3-5].

GBM CSCs are believed to originate from the transformation of neural stem cells of the embryonic matrix and of the neurogenic zones of the adult brain [6], or from the dedifferentiation of hemispheric astrocytes or tumor cells. The latter reacquire stemness through embryonic regression, upon the progressive accumulation of mutations [7-10]. GBM CSCs show self-renewal, clonogenicity and tumorigenicity when transplanted into mice [11]. In culture systems without a coated matrix CSCs occurrence in a tumor is denounced by the generation of neurospheres (NS), beside adherent cells (AC), after the addition of Epidermal Growth Factor (EGF) and basic Fibroblast Growth Factor (bFGF) [12]. GBM CSCs share with neural stem cells stemness antigens, such as CD133, Musashi1, Nestin and SOX2 [12,13], and share the genetic alterations with primary tumors [10,14]. They often show high activity of Transforming Growth Factor/Bone Morphogenetic Protein, Notch, Wnt and Sonic Hedgehog Homolog pathways, which are involved in self-renewal, proliferation and invasion [15].

The molecular basis of chemoresistance in GBM CSCs are under intensive investigation [3,16-18]. The main drugs used in the therapy of GBM are the DNA-damaging agents, such as the alkylating agents temozolomide (TMZ) and carmustine (BCNU), the topoisomerase II inhibitor etoposide, the topoisomerase I inhibitor irinotecan, the DNA-

intercalating drug doxorubicin [2]. TMZ methylates the O^6-position on guanine that mismatches with thymine in genomic DNA. The subsequent DNA aberration blocks replication and induces cell death. It is generally recognized that the over-expression of O^6-methylguanine-DNA methyltransferase (MGMT), which removes the alkyl group from guanine, mediates the resistance to TMZ in GBM [3,19]. However, MGMT alone is not always correlated with resistance to TMZ in GBM CSCs. A plethora of additional intrinsic factors (e.g. the activity of DNA-repairing systems, the activity of specific signaling pathways involved in cell proliferation and apoptosis protection) or extrinsic factors (e.g. the hypoxic environment, the presence of CSCs niches rich of protective growth factors), may contribute to the chemoresistant phenotype of GBM CSCs [3,20].

The role of membrane ATP-binding cassette (ABC) transporters, such as P-glycoprotein (Pgp/ABCB1), Multidrug-resistance Related Protein 1 (MRP1/ABCC1), Breast Cancer Resistance Protein (BCRP/ABCG2), as inducers of the chemoresistant phenotype in GBM CSCs is still matter of debate [3]. Pgp [21,22], MRP1/3/5 [21] and BCRP [23,24] have been found highly expressed in GBM CSCs, either derived from primary tumors [21,23] or obtained *in vitro* by growing AC in the NS-generating medium [22]. The overexpression of Pgp in NS U87-MG cells is predictive of resistance to doxorubicin, etoposide, carboplatin, BCNU [22] and vincristine [25]. TMZ has been reported to be a substrate of Pgp [26], although this observation is still controversial.

To our knowledge, the regulation of ABC transporters in GBM CSCs has not yet been investigated. In this work we found that Pgp levels in GBM CSCs are controlled by Wnt3a oncogene and that clinically achievable doses of TMZ interfere with the Wnt3a-dependent signaling and decrease the expression of Pgp in this tumor population.

Materials and Methods

Chemicals.

Plasticware for cell cultures was from Falcon (Becton Dickinson, Franklin Lakes, NJ). TMZ was obtained from Sigma-Aldrich (St.Louis, MO). WntA or 2-amino-4-(3,4-(methylenedioxy)benzylamino)-6-(3-methoxyphenyl)pyrimidine) was purchased from Calbiochem (San Diego, CA). Human recombinant Dickkopf-1 (Dkk-1) was from R&D Systems (Minneapolis, MN). Electrophoresis reagents were obtained from Bio-Rad Laboratories (Hercules, CA); the protein content of cell lysates was assessed with the BCA kit from Sigma-Aldrich. When not otherwise specified, all the other reagents were purchased from Sigma-Aldrich.

Cells.

Primary human GBM cells (CV17, 01010627, No3) were obtained from surgical samples of patients operated at the Department of Neuroscience, Neurosurgical Unit, Universities of Turin and Novara, Italy, and from DIBIT San Raffaele, Milan, Italy (dr. Rossella Galli). The histological diagnosis was performed according to WHO guidelines. Cells were cultured as NS or AC as previously described [27], with minor modifications. For NS, DMEM-F12 medium was supplemented with 1 M HEPES, 0.3 mg/ml glucose, 75 μg/ml $NaHCO_3$, 2 mg/ml heparin, 2 mg/ml bovine serum albumin, 2 mM progesterone, 20 ng/ml EGF, 10 ng/ml bFGF. For AC, DMEM supplemented with 0.1 ml/ml fetal bovine serum (FBS; Lonza, Basel, Switzerland) was used. U87-MG (ATCC, Rockville, MD) were used as GBM reference cell line for both NS and AC. AC were obtained from dissociated NS cells, centrifuged at 1,200g for 5 min and seeded in AC medium.

Morphological analysis of GBM cells was performed by bright field microscope Zeiss Axiovert 200M (Karl Zeiss, Oberkochen, Germany) equipped with an AxioCam and ICC3 and coupled to an imaging system (AxioVision Release 4.5, Zeiss). For phenotypic

characterization, the following antibodies were used: anti-CD133 (Miltenyi Biotec, Bergisch Gladbach, Germany), anti-nestin (Millipore, Billerica, MA), anti-Musashi-1 (Millipore), anti-SOX2 (R&D Systems), anti-EGF receptor (EGFR; Cell Signaling Technology Inc, Danvers, MA), anti-p53 (Dako, Glostrup, Denmark), anti-glial fibrillary acidic protein (GFAP; Dako), anti-galactocerebroside (Gal-C; Millipore), anti-βIII-tubulin (Millipore), followed by goat anti-rabbit fluorescein-isothiocyanate (FITC)-conjugated IgG and rabbit anti-mouse tetramethyl rhodamine iso-thiocyanate (TRITC)-conjugated IgG antibodies. Nuclei were counterstained with 4',6-diamidino-2-phenylindole (DAPI). The observations were made by immunofluorescence on a Zeiss Axioskop microscope equipped with an AxioCam5MRSc and coupled to an imaging system (AxixoVision Release 4.5, Zeiss), by using a 63 x oil immersion objective (1.4 numerical aperture) and 10 x ocular lens. For each experimental point, a minimum of 5 microscopic fields were examined.

Human doxorubicin-sensitive colon cancer HT29 cells and the doxorubicin-resistant counterpart HT29-dx, generated and cultured as previously reported [28], were chosen as a model of chemosensitive and chemoresistant cells.

Clonogenic and self-renewal assays.

For clonogenic assay, AC and dissociated NS were seeded in 48-wells plate at a concentration of 100 cells/well in the respective medium. Fresh medium was added weekly. At day 14, 28 and 42, the number of spheres or adherent colonies, containing at least 50 cells, was counted by bright field microscopy. Results were expressed as clonogenic index (number of spheres or adherent colonies/100 plated cells). When the clonogenic assay was performed with NS treated with TMZ or other chemotherapeutic drugs, cells were treated at day 4, 11, 18, 25, 32, 39 with 50 μM TMZ for 72 h, with or without the second drug added in the last 24

h, then washed and re-seeded in fresh medium. The number of spheres was counted at day 14, 28 and 42 as reported above.

For self-renewal assay, AC and dissociated NS cells were serially diluted and seeded in 96-wells plate at a concentration ranging from 0.5 to 3 cells/well in the respective medium. 18 h after seeding, the wells actually containing 1 cell were identified by microscope inspection and used for the assay. Fresh medium was added weekly. The number of cells per each well was counted at day 14, 28 and 42.

***In vivo* tumorigenicity.**

Tumorigenicity was tested by transplanting NS and AC into NOD SCID mice (Charles River, Calco, Italy). Two microliters of a 1×10^8 cells/ml suspension were stereotactically injected into the right striatum as previously described [11]. Injections were carried out at the DIBIT San Raffaele, Milan. Formalin-fixed, paraffin-embedded (FFPE) brains were stained with hematoxylin/eosin.

Cell cycle analysis.

Cells were washed twice with fresh PBS, incubated in 0.5 ml ice-cold ethanol (700 µl/ml) for 15 min, then centrifuged at 1,200g for 5 min at 4°C and rinsed with 0.3 ml of citrate buffer (50 mM Na_2HPO_4, 25 mM sodium citrate, 10 µl/ml Triton X-100), containing 10 µg/ml propidium iodide and 1 mg/ml RNAse (from bovine pancreas). After a 15 min incubation in the dark, the intracellular fluorescence was detected by a FACSCalibur flow cytometer (Becton Dickinson). For each analysis, 10,000 events were collected and analyzed by the Cell Quest software (Becton Dickinson).

Cytotoxicity and proliferation assays.

The release of lactate dehydrogenase (LDH) in cell supernatant, considered an index of cells damage and necrosis, was measured as described earlier [28]. Briefly, the extracellular medium was centrifuged at 12,000 g for 15 min to pellet cellular debris, whereas the cells were washed with fresh medium, detached with 0.01% v/v trypsin/EDTA, re-suspended in 0.2 ml of 82.3 mM triethanolamine phosphate-HCl (pH 7.6) and sonicated on ice with two 10 s-bursts. LDH activity was measured in the extracellular medium and in the cell lysate: 50 µl of supernatant from extracellular medium or 5 µl of cell lysate were incubated at 37°C with 5 mM NADH. The reaction was started by adding 20 mM pyruvic acid and was followed for 6 min, measuring absorbance at 340 nm with a Packard EL340 microplate reader (Bio-Tek Instruments, Winooski, VT). The reaction kinetics was linear throughout the time of measurement. Both intracellular and extracellular enzyme activities were expressed as µmol NADH oxidized/min/dish, then extracellular LDH activity was calculated as percentage of the total LDH activity in the dish.

Cell proliferation was measured by growing cells for 24 h in a culture medium containing 1 µCi/ml [^{3}H]thymidine (62 Ci/mmol; Amersham Bioscience, Piscataway, NJ). At the end of the incubation the cells were washed with ice-cold PBS, detached by trypsin/EDTA, and re-suspended in 200 µl PBS. A 50-µl aliquot was used for protein quantification, while the remaining part was counted by liquid scintillation. [^{3}H]thymidine incorporated in each sample was expressed as pmol/mg cell proteins.

Wnt3a overexpression and silencing.

50,000 adherent 010627 cells were transfected with 2 µg Wnt3a-pCMV6-AC-GFP (green fluorescence protein) expression vector (Origene Technologies Inc, Rockville, MD) or pCMV6-AC-GFP empty vector (Origene Technologies Inc) as a control, using Turbofectin 8.0 (Origene Technologies Inc). Cells were sorted 24 h after the transfection by detecting the

GFP-positive cells (FACSCalibur system). Transfected cells (010627 AC Wnt3a$^+$) were re-seeded in fresh AC medium and used for experiments. For Wnt3a silencing, 300,000 neurosphere-forming 010627cells were treated with Turbofectin 8.0 and 1 μg pGFP-V-RS shRNA Wnt3a vector (Origene Technologies Inc.) or a 29-mer scrambled shRNA pGFP-V-RS vector (Origene Technologies Inc.), used as control. 24 h after the transfection, green fluorescent cells were sorted by flow cytometry analysis. Cells (010627 NS Wnt3a$^-$) were then seeded in fresh NS medium and used for the experiments.

Cells were monitored daily by bright field microscopy. Morphological analysis was performed 72 h after the transfection by Olympus FV300 laser scanning confocal microscope equipped with a Blue Argon (488 nm) laser and FluoView 300 software (Olympus Biosystems, Hamburg, Germany). Nomarski images were obtained by differential interference contrast optical components installed on an IX71 inverted microscope. For each experimental point, a minimum of 5 microscopic fields were examined.

Subcultures of 010627 AC Wnt3a$^+$ cells stably overexpressing Wnt3a and 010627 NS Wnt3a$^-$ cells stably silenced for Wnt3a were set up, by selecting cells in neomycin or puromycin-containing medium, respectively. Cells were cultured up to 20 passages in the respective medium. The persistence of the GFP signal was monitored weekly by microscope analysis: samples were rinsed with PBS, fixed with 40 μg/ml paraformaldehyde for 15 min, washed three times with PBS and incubated with DAPI for 3 min at room temperature in the dark. Cells were washed three times with PBS and once with water, then the slides were mounted with 4 μl of Gel Mount Aqueous Mounting and examined with a Leica DC100 fluorescence microscope (Leica Microsystems GmbH, Wetzlar, Germany). For each experimental point, a minimum of 5 microscopic fields were examined. In parallel, a subculture of 010627 AC Wnt3a$^+$ cells grown in NS medium and a subculture of 010627 NS

Wnt3a$^-$ cells grown in AC medium were set up and maintained for 20 passages; cell morphology was analyzed as reported above.

Quantitative Real Time (qRT)-PCR.

Total RNA was extracted and reverse-transcribed using the QuantiTect Reverse Transcription Kit (Qiagen, Hilden, Germany). qRT-PCR was carried out using IQ^{TM} SYBR Green Supermix (Bio-Rad), according to the manufacturer's instructions. The same cDNA preparation was used for the quantitation of the genes of interest and β-actin, used as an housekeeping gene. Primer sequences are reported in Supplementary Table 1. The relative quantitation was performed by comparing each PCR product with the housekeeping PCR product, using the Bio-Rad Software Gene Expression Quantitation (Bio-Rad).

Promoter methylation assays.

Wnt3a and *ABCB1* promoter sequences were obtained by UCSC Genome Browser (http://genome.ucsc.edu/). The CpG islands localization on *Wnt3a* and *ABCB1* promoters and the design of primers for Methylation Specific PCR (MSP) was performed with the Methprimer software (http://www.urogene.org/methprimer). Primers specific for immunoprecipitation and ELISA of *Wnt3a* promoter were designed with Primer3 software (http://frodo.wi.mit.edu/primer3). The primer sequences are reported in Supplementary Table 1.

For immunoprecipitation and ELISA assays, 10 ng of extracted genomic DNA were amplified with specific primers for the CpG islands-rich region of the *Wnt3a* promoter, using the KlenTaq LA DNA Polymerase (Sigma-Aldrich). The 1,133 bp PCR product was purified with the GenElute™ PCR Clean-Up (Sigma-Aldrich) and divided into aliquots of 100 ng. One aliquot was immunoprecipitated overnight at 4°C with 1 μg of an anti-5 methyl cytosine

(5mC) antibody (Active Motif, La Hulpe, Belgium), using the Magna ChIP™ A/G Chromatin Immunoprecipitation Kit (Millipore). Samples were washed, the immunoprecipitated DNA was eluted using the GenElute Mammalian Genomic DNA Miniprep Kit (Sigma-Aldrich) and resolved on agarose gel stained with ethidium bromide. A second aliquot was subjected to the quantification of 5mC, using the 5mC DNA ELISA Kit (Zymo Research, Irvine, CA), following the manufacturer's instruction. The absorbance of each sample was read at 450 nm using a Packard EL340 microplate reader and converted into percentage of 5mC, according to a titration curve prepared with serial dilutions of the 5mC DNA positive control provided with the kit.

For MSP assay, 1 μg of extracted genomic DNA was subjected to bisulfite modification using the Methyl Easy Xceed kit (Human Genetics Signatures, Randwick, Australia), following the manufacturer's instruction. MSP was performed with AmpliTaq Gold DNA Polymerase (Applied Biosystems, Carlsbad, CA), including universally methylated (CpGenome, Millipore) and unmethylated DNA samples (Human Genetics Signatures) as controls. PCR products were visualized on agarose gel stained with ethidium bromide.

Western blot analysis.

Cells were rinsed with lysis buffer (50 mM Tris-HCl, 1 mM EDTA, 1 mM EGTA, 150 mM NaCl, 10μl/ml Triton-X100; pH 7.4), supplemented with the protease inhibitor cocktail set III (80 μM aprotinin, 5 mM bestatin, 1.5 mM leupeptin, 1 mM pepstatin; Calbiochem), 2 mM phenylmethanesulfonylfluoride and 1 mM Na_3VO_4, then sonicated and centrifuged at 13,000g for 10 min at 4^{o}C. 20 μg protein extracts were subjected to SDS-PAGE and probed with the following antibodies: anti-MGMT (NeoMarkers, Fremont, CA, USA); anti-Wnt3a (Abcam, Cambridge, UK); anti-GSK3 (BD Biosciences, Franklin Lakes, NJ); anti-

phospho(Tyr216)GSK3 (BD Biosciences); anti-β-catenin (BD Biosciences); anti-phospho(Ser33/37/Thr41)β-catenin (Cell Signaling Technology Inc); anti-Pgp/ABCB1 (C219; Calbiochem); anti-tubulin (Santa Cruz Biotechnology Inc, Santa Cruz, CA), followed by the peroxidase-conjugated secondary anti-mouse or anti-rabbit antibody (Bio-Rad). The membranes were washed with TBS/Tween and proteins were detected by enhanced chemiluminescence (PerkinElmer, Waltham, MA).

Cytosol/nucleus separation was performed as reported [29]. 10 μg of cytosolic or nuclear extracts were subjected to Western blot analysis using the anti-β-catenin antibody. To check the equal control loading in cytosolic and nuclear fractions, samples were probed respectively with an anti-tubulin or an anti-TATA-box binding protein (TBP/TFIID) antibody (Santa Cruz Biotechnology Inc).

Flow cytometry analysis.

Cells were washed with PBS, detached with Cell Dissociation Solution (Sigma-Aldrich) and re-suspended at 5×10^5 cells/m1 in culture medium containing 50 μl/ml FBS. Samples were washed with 2.5 μg/ml BSA-PBS, incubated with the primary antibodies for Frizzled (Santa Cruz Biotechnology Inc.) or LRP6 (Abcam) for 45 min at 4°C, then washed twice and incubated with the secondary FITC-conjugated antibody for 30 min at 4°C. After washing and fixation in paraformaldehyde 20 μg/ml, the surface amount of Frizzled or LRP6 was detected on 100,000 cells by a FACSCalibur system, using the Cell Quest software (Becton Dickinson). Control experiments included incubation of cells with non-immune isotypic antibody, followed by secondary antibody.

Chromatin Immunoprecipitation (ChIP).

ChIP experiments were performed using the Magna ChIP™ A/G Chromatin Immunoprecipitation Kit. Samples were immunoprecipitated with 5 μg of anti-β-catenin antibody or with no antibody. The immunoprecipitated DNA was then washed and eluted twice with 100 μl elution buffer (0.1 M $NaHCO_3$, 10 μl/ml SDS), the cross-linking was reversed incubating the samples at 65°C for 6 h, then samples were incubated with proteinase K for 1 h at 55°C. The DNA was eluted using the GenElute Mammalian Genomic DNA Miniprep Kit and analyzed by PCR. The putative β-catenin site on *ABCB1* promoter was validated with the MatInspector software (http://www.genomatix.de/; Munich, Germany). The primers sequences, designed with Primer3 software (http://frodo.wi.mit.edu/primer3), are reported in Supplementary Table 1. PCR products were visualized on agarose gel stained with ethidium bromide. As negative internal controls, immunoprecipitated samples were subjected to PCR with primers matching 10,000 bp upstream the *ABCB1* promoter. In this condition no PCR product was detected (not shown).

Rhodamine 123 efflux.

The efflux of rhodamine 123, a specific substrate of Pgp [30], was taken as index of Pgp activity. Cells were then washed with fresh PBS, detached with Cell Dissociation Solution and re-suspended at 5 x 10^5 cells/ml in 1 ml of culture medium. The samples were maintained at 37°C for 20 min in the presence of 1 μg/ml rhodamine 123. After this incubation time, cells were washed and re-suspended in 0.5 ml of PBS; the intracellular rhodamine content, which is inversely related to its efflux, was detected using a FACSCalibur system (Becton Dickinson). For each analysis 100,000 events were collected. Data were analyzed by the CellQuest software (Becton Dickinson).

Statistical analysis.

All data in text and figures are provided as means ± SD. The results were analyzed by a one-way Analysis of Variance (ANOVA). A $p < 0.05$ was considered significant.

Results

Temozolomide chemosensitizes GBM stem cells to other anticancer drugs.

We used three GBM cell cultures (CV17, 010627 and U87-MG), grown both as AC or NS, depending on the culture conditions (Fig. 1A), and we analyzed clonogenicity, self-renewal, cell cycle distribution and *in vivo* tumorigenicity. For all three cell lines, NS were significantly more clonogenic than AC (Fig. 1B); when plated at a concentration of 1 cell/well, AC did not duplicate over a period of 42 days, differently from NS (Fig. 1C). 010627 NS were the most active in clonogenic and self-renewal assay, followed by U87-MG and CV17. Compared with NS, AC showed a significantly higher percentage of cells arrested in G2-phase and a significantly lower percentage of cells in S-phase (Fig. 1D).

The *in vivo* tumorigenicity of 010627 and U87-MG NS has been already reported [11]. As far as CV17 cells are concerned, upon intracranial transplantation, AC did not develop tumors (Supplementary Fig. S1A) or showed a reduced tumorigenicity in two out of four cases (data not shown), whereas NS developed tumors (Supplementary Fig. S1B), demonstrating that NS populations included true GBM SCs.

The distribution of stemness and differentiation markers revealed that 010627 NS expressed more stemness markers (CD133, Musashi-1, Nestin, SOX2) than the other NS (Supplementary Table 2). MGMT was detected in CV17 NS and AC, but not in 010627 and U87-MG cells (Supplementary Fig. S2).

TMZ for 72 h (Fig. 2A) or 120 h (not shown) induced a dose-dependent cell death, measured as release of intracellular LDH in the extracellular medium, in AC but not in NS, except for U87-MG cells at the highest concentration (200 μM). Doxorubicin, a drug

effective against GBM cells [31], was cytotoxic in AC, as well as in doxorubicin-sensitive human colon cancer HT29 cells, not in NS and in the doxorubicin-resistant cell line HT29-dx (Fig. 2B). Surprisingly, the pre-incubation with an apparently non toxic (50 μM) concentration of TMZ for 72 h, followed by doxorubicin in the last 24 h, induced cell death in NS, not observed with each drug used alone (Fig. 2C). Weekly administration of TMZ or doxorubicin did not reduce the clonogenic potential of NS (Fig. 2D); only the pre-treatment with TMZ for 72 h, with further addition of doxorubicin in the last 24 h, significantly decreased clonogenicity (Fig. 2D). Although devoid of effect in cytotoxicity and clonogenicity assay, 50 μM TMZ for 72 h was sufficient to induce a G2-arrest, an effect already documented for this drug [32], and a significant increase of pre-G1 cells, suggestive of apoptotic cells, in the case of CV17 NS (Fig. 2E). On the contrary, doxorubicin, which was also expected to induce a G2-arrest in sensitive tumor cells [33], was not effective in NS. The combination of TMZ followed by doxorubicin significantly increased the percentage of cells arrested in G2-phase and decreased the percentage of cells in S phase, towards untreated NS or NS treated with TMZ alone (Fig. 2E).

The synergistic effects in terms of cell damage (Fig. 3A), reduced clonogenicity (Fig. 3B) and cell cycle arrest (Fig. 3D) were observed also when TMZ was followed by vinblastine or etoposide, but not by cisplatin (Supplementary Fig. S3), methotrexate (Supplementary Fig. S4) or mitoxantrone (Supplementary Fig. S5). Of note, the drugs that synergized with TMZ (doxorubicin, vinblastine and etoposide) were all substrates of Pgp, whereas cisplatin, methotrexate and mitoxantrone are mainly effluxed by MRP1/2 and BCRP [34].

Temozolomide down-regulates *Wnt3a* in GBM stem cells.

Since TMZ chemosensitizes specifically NS to Pgp substrates, we first investigated whether in this population there was a correlation between the expression of typical stemness antigens, like Notch, SHH and Wnts, and the expression of Pgp. *Notch 1, 2, 3, 4* and *Sonic Hedgehog* were variably present in CV17, 010627 and U87-MG cells, but their expression did not change in an univocal way between AC and NS (Supplementary Fig. S6A-B). Among the Wnt antigens present in neural stem cells [35], *Wnt5* mRNA was poorly detectable, whereas *Wnt3a* was higher in all the NS cultures compared with AC (Fig. 4A). NS showed greater expression of *ABCB1*(Fig. 4B), which encodes for Pgp, compared with AC and TMZ strongly decreased both *Wnt3a* and *ABCB1* expression in NS in a time-dependent way (Fig. 4C). NS also had an higher expression of *ABCC1* and *ABCG2* (Supplementary Figure S7A-B), but they were not affected by TMZ (Supplementary Fig. S7C).

The decrease of *Wnt3a* started earlier (i.e. at 24 h) than the decrease of *ABCB1* (Fig. 4C), leading to hypothesize that a "priming" event induced by TMZ may occur on *Wnt3a* gene rather than on *ABCB1* gene. Methylation of CpG islands in promoters is an effective mechanism of gene down-regulation. Of note, *Wnt3a* promoter has many CpG islands, whereas *ABCB1* promoter has none (Supplementary Fig. S8A-B). We thus analyzed how was the methylation of *Wnt3a* promoter in GBM stem cells untreated and treated with TMZ. The fragment rich of CpG islands in *Wnt3a* promoter was amplified by PCR from 010627 NS and subjected to immunoprecipitation with a specific anti 5mC antibody: untreated cells did not show any detectable band of DNA containing 5mC, which instead became detectable after TMZ treatment (Supplementary Fig. S9A). Similarly, using an ELISA kit which allowed the quantification of 5mC contained in *Wnt3a* promoter, the percentage of 5mC was below 1% in 010627 NS, but increased up to 25% in cells treated with TMZ (Supplementary Fig. S9B). Interestingly, the co-incubation with 5-aza-2'-deoxycytidine, an agent that inhibits the methylation of cytosine on position 5 exerted by DNA methyl transferases, significantly

counteracted the TMZ effects (Supplementary Fig. S9A-B). In keeping with these experimental findings, in all the NS lines analyzed with methylation specific PCR (MSP) we found a fully unmethylated promoter of *Wnt3a*, which became methylated in the presence of TMZ (Fig. 4D). TMZ effect was drug-specific: another alkylating agent, BCNU, did not change the expression levels of *Wnt3a* and *ABCB1* (Supplementary Fig. S10A), irrespectively of its cytotoxicity (Supplementary Fig. S10B). 010627 adherent cells had low *Wnt3a* basal expression and we did not detect any further reduction nor change in promoter methylation by TMZ (data not shown).

Wnt3a controls morphology, proliferation and *ABCB1* expression in GBM stem cells.

To correlate the expression changes of *Wnt3a* with the ones of *ABCB1*, we overexpressed Wnt3a in 010627 AC (creating the 010627 AC Wnt3a$^+$ subline) and silenced Wnt3a in NS 010627 cells (generating the 010627 NS Wnt3a$^-$ subline), using specific vectors containing a reporter GFP. The transfected populations were identified by flow-cytometry (Fig. 5A), the effective overexpression or silencing of *Wnt3a* was checked by qRT-PCR (Fig. 5B). Surprisingly, 72 h after the transfection, 010627 AC Wnt3a$^+$ started to detach and grow as NS, whereas 010627 NS Wnt3a$^-$ progressively disaggregated and grew as single-cell or few-cell suspension (Fig. 5C). The morphology (Supplementary Fig. S11A) and the expression levels of Wnt3a (Supplementary Fig. S11B) in 010627 AC Wnt3a$^+$ cells stably overexpressing Wnt3a and in 010627 NS Wnt3a$^-$ cells stably silenced for Wnt3a were checked up to 20 passages, without observing any further modifications. Of note, 010627 AC Wnt3a$^+$ cells grew as NS in NS and AC media, 010627 NS Wnt3a$^-$ grew as single-cell/few-cells suspension in both media (data not shown). Wild-type NS 010627 cells grew faster than AC (Fig. 5D); 010627 AC Wnt3a$^+$ proliferated even faster than wild-type 010627 NS, whereas in 010627 NS Wnt3a$^-$ cells the proliferation rate was dramatically reduced (Fig. 5D).

In keeping with this trend, 010627 AC Wnt3a$^+$ showed a greater clonogenic potential than wild-type 010627 AC; the clonogenicity was even higher than that of wild-type 010627 NS (Fig. 5E). On the contrary, 010627 NS Wnt3a$^-$ had a dramatic decrease in their clonogenic potential, and displayed a similar behavior to wild-type 010627 AC (Fig. 5E). Wild-type 010627 AC did not self-duplicate, but acquired self-renewal capacity - even higher than wild-type 010627 NS - when overexpressing Wnt3a (Fig. 5F). By contrast, in 010627 NS Wnt3a$^-$ the self-renewal, which was a typical feature of NS, was dramatically reduced. However 010627 NS Wnt3a$^-$ did not lose completely the self-renewal potential: at day 42 we detected 1 cell in 5/10 wells, 2 cells in 3/10 wells, 4 cells in 2/10 wells (Fig. 5F).

Wnt signaling is canonically transduced by the Frizzled receptors and the LDL-receptor related protein (LRP)-5 and -6 co-receptors; in the absence of Wnt, cytosolic β-catenin bound to APC/axin complex is phosphorylated by glycogen synthase kinase-3 (GSK3) and ubiquitinated. Wnt reduces the phosphorylation of β-catenin by GSK3 and allows its translocation into the nucleus [37,38], where it associates with T-cell factor/lymphoid enhancer factors and acts as a transcription activator of several target genes, including *ABCB1* [39]. Both 010627 wild-type NS and 010627 AC Wnt3a$^+$ had low or undetectable levels of active phospho(Tyr216)GSK3 and of phospho(Ser33/37/Thr41)β-catenin (Fig. 6A). On the contrary, in 010627 wild-type AC and 010627 NS Wnt3a$^-$, phospho(Tyr216)GSK3 and phospho(Ser33/37/Thr41)-β-catenin were high (Fig. 6A). Of note for the aim of this work, transient (Figure 6B) and stably transfected (Supplementary Fig. S11C) 010627 AC Wnt3a$^+$ had higher levels of *ABCB1* than parental 010627 AC, whereas 010627 NS Wnt3a$^-$ had lower levels of *ABCB1* than parental 010627 NS (Fig. 6B; Supplementary Fig. S11C).

Temozolomide down-regulates *ABCB1* transcription by interfering with the Wnt3a/GSK3/β-catenin pathway in GBM stem cells.

Since TMZ decreases the *ABCB1* levels, we investigated whether this effect was consequent to the disruption of Wnt3a/GSK3/β-catenin axis. All AC had no detectable amounts of Wnt3a and constitutive expression of phospho(Tyr216)GSK3 and phospho(Ser33/37/Thr41)β-catenin; TMZ did not change this expression pattern (Fig. 7A). In NS Wnt3a was basally expressed, and was paralleled by low levels of phospho(Tyr216)GSK3 and phospho(Ser33/37/Thr41)β-catenin. TMZ, that reduced Wnt3a levels, increased the amount of phosphorylated GSK3 and β-catenin (Fig. 7A). NS had also higher amounts of the Wnt3a-receptor Frizzled (Supplementary Fig. S12A) and co-receptor LRP6 (Supplementary Fig. S12B) compared to AC. Since TMZ did not modify the surface levels of Frizzled or LRP6 (Supplementary Fig. S12A-B), we excluded that the drug interfered at this point in Wnt3a axis.

Untreated NS displayed β-catenin translocated into the nucleus (Fig. 7B), where it was bound to the *ABCB1* promoter (Fig. 7C). In keeping with the increased activation of GSK3 and phosphorylation of β-catenin, TMZ dramatically reduced the amount of β-catenin detectable in NS nuclear extracts (Fig. 7B) and decreased the binding on *ABCB1* promoter (Fig. 7C).

To further confirm that TMZ decreased the transcription of *ABCB1* by disrupting the Wnt3a/GSK3/β-catenin axis, we treated 010627 NS with known activators and inhibitors of the Wnt3a/GSK3/β-catenin pathway and measured the expression of *ABCB1* mRNA: the synthetic Wnt activator WntA and the GSK3 inhibitor LiCl indeed increased *ABCB1* expression, whereas the recombinant Dkk-1 protein decreased it. TMZ counteracted the effects of both WntA and LiCl (Supplementary Fig. S13).

Temozolomide decreases expression ad activity of Pgp and restores the cytotoxicity of Pgp substrates in GBM stem cells.

CV17, 010627 and U87-MG NS had detectable amounts of Pgp protein, which was strongly reduced by TMZ (Fig. 8A). As a consequence, the intracellular accumulation of rhodamine 123, a specific substrate of Pgp, was basally low in NS (Fig. 8B). Of note, TMZ was as effective as the Pgp inhibitors verapamil and cyclosporine A in reducing the efflux of rhodamine 123 (Fig. 8B). In keeping with this trend, verapamil and cyclosporine A, which were not cytotoxic in NS, restored the cytotoxicity of the Pgp substrates doxorubicin, vinblastine and etoposide (Fig.8C), achieving the same efficacy of non toxic doses of TMZ (Fig. 2C and 3A).

Discussion

One of the most severe problems encountered by chemotherapy against GBM is the high chemoresistance of the CSCs component. We addressed this point investigating GBM cultures (derived from primary tumors or from commercially available cells), grown as AC and NS. The latter were used as models of GBM CSCs, according to our results of clonogenic and self-renewal assays, *in vivo* tumorigenicity, and to the literature [9,11,12,13,40]. A strong *in vitro* resistance towards a panel of drugs, which have been variably used in GBM therapy [2], differentiates NS from AC, suggesting that they may represent two different grades of GBM malignancy. Also our NS showed a multidrug-resistant phenotype. When treated with TMZ, then washed and re-seeded in fresh medium, NS did not alter their proliferation rate. This suggests that adequate recovery periods after TMZ pulses allow cells surviving to TMZ treatment to restart proliferation. This observation is in accord with another work showing that 200 μM TMZ for 7 days, followed by a recovery period of 7 days in fresh medium, did not prevent the formation of secondary spheres of U87-MG NS and the tumor formation *in vivo* [41]. Of note, the resistance to TMZ in our models was independent of MGMT levels, since it occurred in both MGMT-positive and MGMT-negative cells, suggesting that several

other factors are likely involved [3,20]. Unexpectedly, however, non cytotoxic doses of TMZ chemosensitized NS to apparently non cytotoxic doses of doxorubicin, vinblastine and etoposide, in terms of cell damages, decreased clonogenic potential and cell cycle arrest.

Polichemotherapy protocols have been variously experimented in GBM [2]; for instance, TMZ achieves an appreciable synergistic effect when used together with drugs (e.g. inhibitors of poly-ADP ribosyltransferase) that hamper the DNA-repairing machinery [2]. In our study, the drugs that synergize with TMZ have other targets than the DNA-repairing enzymes, indicating that the molecular basis of the synergism should rely on different reasons. Doxorubicin, vinblastine and etoposide are all substrates of Pgp [34]. By contrast, no synergism was observed between TMZ and drugs that are not substrates of Pgp. Overall, these results suggest that, in our experimental conditions, the actual responsible of the decreased proliferation of NS was not TMZ, but the second chemotherapeutic drug, when it is substrate of Pgp. This observation led us to investigate how TMZ can sensitize GBM CSCs to Pgp substrates and how Pgp is regulated in GBM CSCs, an issue that has been poorly explored.

In keeping with other works [21,22], NS showed a higher expression of *ABCB1* than AC. Of note, TMZ down-regulated *ABCB1* levels, without affecting other ABC transporters. Looking for factors highly expressed in GBM CSCs and putative controllers of *ABCB1*, we found that NS had higher levels of *Wnt3a* compared with AC. Intriguingly, TMZ reduced *Wnt3a* expression. The decreased expression of *Wnt3a* was associated to an increased amount of 5mC in the CpGs islands of *Wnt3a* promoter. The cytotoxic effects of TMZ as alkylating agent are due to the methylation of guanine on O^6 position, an event that induces DNA strand breaks if not repaired by MGMT enzyme. The vast majority of methylation events exerted by TMZ are however represented by other methylations, which are usually not cytotoxic [36]. The consequences of these non toxic methylations, as well as the molecular mechanisms involved,

have been less investigated. To the best of our knowledge there are no reports showing that TMZ directly methylates cytosine on 5 position. Interestingly we observed that the increase of 5mC induced by TMZ was reversed by the DNA methyl transferases inhibitor 5-aza-2'-deoxycytidine. Such observation suggests that the methylation changes exerted by TMZ are likely due to indirect mechanisms; for instance, they might be consequent to changes in DNA methyltransferases activity, produced by TMZ or its metabolites. Our results pave the way to further investigations, aimed to clarify the molecular mechanism by which TMZ may modulate DNA methyltransferases activity or expression, and to unveil which intracellular factors (e.g. the abundance of CpG islands, the accessibility of the position 5 of cytosine after the chromatin folding process, the absence or presence of DNA-binding proteins on a specific promoter, the type and activity of DNA methyltransferases and demethylating enzymes) are important to determine the rate and type of methylations exerted by TMZ.

In the specific case of *Wnt3a*, its decrease is achieved by TMZ concentrations that are not sufficient to induce a significant cells death in NS, but are compatible with the levels of TMZ circulating in blood [42]. We can speculate that also low doses of TMZ have a benefit, e.g. by down-regulating a gene like *Wnt3a*, which is crucial for cell growth, tumorigenesis and stemness maintenance in GBM [43,44].

As suggested by *Wnt3a* silencing and overexpression experiments, changes in Wnt3a amount produced wide phenotypic changes in GBM CSCs. Since in our model the only overexpression of Wnt3a was sufficient to transform the 010627 AC into NS, this finding supports the hypothesis that GBM CSCs may derive from a de-differentiation of tumor cells [7,8]. Moreover, since 010627 AC $Wnt3^+$ cells grew as NS independently from the culture medium, this observation suggests that the transition from AC to NS is mainly driven by endogenous tumor-dependent factors, like Wnt3a signaling. On the other hand, the transition from NS to AC appears more complex, as pointed out by 010627 NS $Wnt3a^-$ cells, which lost

the ability to form neurospheres, but did not acquire the morphologic feature of AC even if cultured in the AC medium. Therefore, also for the transition from NS to AC, intracellular rather than extracellular factors seem having the predominant role. Wnt3a is a major determinant in the acquisition or maintenance of stemness, because when overexpressed it conferred to AC cells a "stemness phenotype" in terms of clonogenicity and self-renewal, even more pronounced than that of NS. However Wnt3a cannot be regarded as the only factor important for stemness, since its silencing was not sufficient to abrogate the self-renewal property or induce a complete transition from NS into AC.

Beside the changes in proliferation and morphology, the decrease of *Wnt3a*, obtained either by gene silencing or by TMZ, lowered the expression of *ABCB1*. Time-dependence experiments with TMZ suggested that the decrease of *Wnt3a* was temporally antecedent to the one of *ABCB1,* raising two questions: 1) does Wnt3a control Pgp expression in GBM CSCs?; 2) does TMZ chemosensitize GBM CSCs to Pgp substrates, by triggering the Wnt3a decrease?

Compared with AC, our GBM NS had higher expression of Frizzled and LRP-6: this situation may favor the basal higher activity of Wnt/β-catenin pathway and the higher basal expression of Pgp. TMZ did not modify the levels of Frizzled and LRP-6, but reduced the production of Wnt3a protein by NS themselves. We suggest that - by doing so - it disrupts a sort of autocrine loop, which may be important for stemness, proliferation and chemoresistance at the same time. To the best of our knowledge these are the first evidences showing that Wnt3a simultaneously controls these features in GBM and that TMZ interferes with this putative Wnt3a loop.

Some experimental evidences correlated Wnt signaling with chemoresistance [39,45,46]. In human multiple myeloma, a tumor that is strongly refractory to several anticancer drugs, autocrine Wnt3a is responsible for chemoresistance; in this case the so-called non canonical

Wnt3a pathway (that recognizes RhoA/RhoA-kinase as intracellular transducers) has a predominant role compared to the GSK3/β-catenin pathway [46]. This work suggests that the downstream effectors may vary, whereas Wnt3a appears as a common upstream inducer of chemoresistance in different tumors. The Wnt antagonist Dkk-1 chemosensitized U87-MG cells to alkylating agents such as BCNU and cisplatin, increasing the sensitivity to DNA damage [45]. A specific effect on Pgp was not described in this paper, which was entirely performed on AC. In our hands AC revealed a very low expression of *ABCB1*. So far, the Pgp-independent effect of Dkk-1 reported in Shou *et al.* is not surprising and can be compatible with our findings on NS, where Pgp levels were high and Dkk-1 down-regulated the expression of *ABCB1*.

Overall, we suggest that TMZ has the peculiar effect to decrease the autocrine production of Wnt3a in GBM CSCs, to increase the phosphorylation of β-catenin and to reduce the β-catenin-induced expression of Pgp. As a consequence, in cells primed by TMZ, Pgp substrates (like doxorubicin, vinblastine and etoposide) can accumulate within resistant tumor cells and reach sufficient concentrations to exert cytotoxic and anti-proliferative effects. Of note, TMZ achieved the same efficacy of Pgp inhibitors, such as verapamil and cyclosporin A, in chemosensitizing GBM CSCs to Pgp substrates. The use of Pgp inhibitors is a useful tool to demonstrate *in vitro* the role of Pgp as a critical factor that makes GBM CSCs resistant to several anticancer drugs. Most of the classical Pgp inhibitors have low specificity and high toxicity *in vivo* and fail in clinical trials. TMZ may represent a valid alternative to these inhibitors, because it has the dual property of being a chemotherapeutic drug and a chemosensitizer agent. Notably, it shows this property at apparently non-cytotoxic and clinically achievable doses. Thus, new treatment schemes, based on the association of TMZ with drugs such as doxorubicin, vinblastine or etoposide, can be hypothesized. The

added value of such associations relies on the specific targeting of GBM CSCs, which are the most resistant and unresponsive component of the tumor.

Funding.

Compagnia di San Paolo "Programma Neuroscienze" (grant 2008.1136); Italian Association for Cancer Research (MFAG 11475); Italian Ministry of University and Research (Programma "Futuro in Ricerca" FIRB 2012). Joanna Kopecka is the recipient of a "Mario and Valeria Rindi" fellowship from Italian Foundation for Cancer Research (FIRC).

Acknowledgments.

We are grateful to Costanzo Costamagna (Department of Oncology, University of Turin) for the technical assistance provided, to Dr. Erika Ortolan (Department of Medical Sciences, University of Turin) for the assistance in confocal microscope analysis and to Dr. Oriana Monzeglio (Neuro-bio-oncology Center, Policlinico di Monza Foundation), for the help with methylation promoter assay. We are indebted with Dr. Michele Lanotte (Department of Neuroscience, Neurosurgical Unit, University of Turin) and with Dr. Rossella Galli (San Raffaele Scientific Institute, Milan) for having provided the primary glioblastoma samples.

References

1. Adamson C, Kanu OO, Mehta AI, et al. GBM multiforme: a review of where we have been and where we are going. *Expert Opin Investig Drugs* 2009;18: 1061–1083.
2. Bai RY, Staedke V, Riggins GJ. Molecular targeting of GBM: Drug discovery and therapies. *Trends Mol Med* 2011;17:301–312.

3. Beier D, Schulz JB, Beier CP. Chemoresistance of glioblastoma cancer stem cells--much more complex than expected. *Mol Cancer* 2011,10:128.

4. Gong X, Schwartz PH, Linskey ME, Bota DA. Neural stem/progenitors and glioma stem-like cells have differential sensitivity to chemotherapy. *Neurology* 2011;76:1126–1113.

5. Yamada R, Nakano I. Glioma stem cells: their role in chemoresistance. *World Neurosurg* 2012;77:237–40.

6. Walton NM, Snyder GE, Park D, Kobeissy F, Scheffler B, Steindler DA. Gliotypic neural stem cells transiently adopt tumorigenic properties during normal differentiation. *Stem Cells* 2009;27:280–289.

7. Stiles CD, Rowitch DF. Glioma stem cells: a midterm exam. *Neuron* 2008;58:832–845.

8. Vescovi AL, Galli R, Reynolds BA. Brain tumour stem cells. *Nat Rev Cancer* 2006;6:425–436.

9. Germano I, Swiss V, Casaccia P. Primary brain tumors, neural stem cell, and brain tumor cancer cells: Where is the link? *Neuropharmacology* 2010;58:903–910.

10. Caldera V, Mellai M, Annovazzi L, et al. Antigenic and Genotypic Similarity between Primary GBMs and Their Derived Neurospheres. *J Oncol* 2011;2011:314962.

11. Galli R, Binda E, Orfanelli U, et al. Isolation and characterization of tumorigenic, stem-like neural precursors from human GBM. *Cancer Res* 2004;64:7011–7021.

12. Gunther HS, Schmidt NO, Phillips HS, et al. GBM-derived stem cell-enriched cultures form distinct subgroups according to molecular and phenotypic criteria. *Oncogene* 2008;27:2897–2909.

13. Christensen K, Schroder HD, Kristensen BW. CD133 identifies perivascular niches in grade II-IV astrocytomas. *J Neurooncol* 2008;90:157–170.

14. Lee J, Kotliarova S, Kotliarov Y, et al. Tumor stem cells derived from GBMs cultured in bFGF and EGF more closely mirror the phenotype and genotype of primary tumors than do serum-cultured cell lines. *Cancer Cell* 2006;9:391–403.

15. Clark P, Treisman DM, Ebben J, Kuo JS. Developmental Signaling Pathways in Brain Tumor-Derived Stem-Like Cells. *Dev Dyn* 2007;236:3297–3308.

16. Eramo A, Ricci-Vitiani L, Zeuner A, et al. Chemotherapy resistance of GBM stem cells. *Cell Death Differ* 2006;13:1238−1241.

17. Ghods AJ, Irvin D, Liu G, et al. Spheres isolated from 9L gliosarcoma rat cell line possess chemoresistant and aggressive cancer stem-like cells. *Stem Cells* 2007;25:1645−1653.

18. Johannessen TCA, Wang J, Skaftnesmo KO, et al. Highly infiltrative brain tumours show reduced chemosensitivity associated with a stem cell-like phenotype. *Neuropathol Appl Neurobiol* 2009;35:380–393.

19. Kaina B, Christmann M, Naumann S, Roos WP. MGMT: key node in the battle against genotoxicity, carcinogenicity and apoptosis induced by alkylating agents. *DNA Repair (Amst)* 2007;6:1079–1099.

20. Johannessen TCA, Prestegarden L, Grudic A, Hegi ME, Bølge Tysnes B, Bjerkvig R. The DNA repair protein ALKBH2 mediates temozolomide resistance in human glioblastoma cells. *Neuro Oncol* 2013; 15:269–278.

21. Salmaggi A, Boiardi A, Gelati M, et al. GBM-Derived Tumorospheres Identify a Population of Tumor Stem-Like Cells with Angiogenic Potential and Enhanced Multidrug Resistance Phenotype. *Glia* 2006;54:850–860.

22. Nakai E, Park K, Yawata T, et al. Enhanced MDR1 Expression and Chemoresistance of Cancer Stem Cells Derived from GBM. *Cancer Invest* 2009;27:901–908.

23. Liu G, Yuan X, Zeng Z, et al. Analysis of gene expression and chemoresistance of CD133+ cancer stem cells in GBM. *Mol Cancer* 2006;5:e67.

24. Bleau AM, Huse JT, Holland EC. The ABCG2 resistance network of GBM. *Cell Cycle* 2009;8:2937–2945.

25. Balik V, Mirossay P, Bohus P, Sulla I, Mirossay L, Sarissky M. Flow Cytometry Analysis of Neural Differentiation Markers Expression in Human GBMs May Predict Their Response to Chemotherapy. *Cell Mol Neurobiol* 2009;29:845–858.

26. Schaich M, Kestel L, Pfirrmann M, et al. A MDR1 (ABCB1) gene single nucleotide polymorphism predicts outcome of temozolomide treatment in GBM patients. *Annal Oncol* 2009;20:175−181.

27. Reynolds BA, Tetzlaff W, Weiss S. A multipotent EGF-responsive striatal embryonic progenitor cell produces neurons and astrocytes. *J Neurosci* 1992;12:4565–4574.

28. Riganti C, Miraglia E, Viarisio D, et al. Nitric oxide reverts the resistance to doxorubicin in human colon cancer cells by inhibiting the drug efflux. *Cancer Res* 2005;65:516–525.

29. Campia I, Gazzano E, Pescarmona G, Ghigo D, Bosia A, Riganti C. Digoxin and ouabain increase the synthesis of cholesterol in human liver cells. *Cell Mol Life Sci* 2009;66:1580−1594.

30. Sarkadi B, Homolya L, Szakacs G, Varadi A. Human Multidrug Resistance ABCB and ABCG Transporters: Participation in a Chemoimmunity Defense System. *Physiol Rev* 2006;86:1179−1236.

31. Hau P, Fabel K, Baumgart U, et al. Pegylated liposomal doxorubicin-efficacy in patients with recurrent high-grade glioma. *Cancer* 2004;100:1199–1207.

32. Chalmers AJ, Ruff EM, Martindale C, Lovegrove N, Short SC. Cytotoxic effects of temozolomide and radiation are additive- and schedule-dependent. *Int J Radiation Oncology Biol Phys* 2009;75:1511–1519.

33. Ling YE, El-Naggar AK, Priebe W, Perz-Soler R. Cell cycle-dependent cytotoxicity, G2/M phase arrest, and disruption of p34cdc2/cyclin B1 activity induced by doxorubicin in synchronized P388 cells. *Mol Pharmacol* 1996;49:832–841.

34. Gottesman MM, Fojo T, Bates SE. Multidrug resistance in cancer: role of ATP-dependent transporters. *Nat Rev Cancer* 2002;2:48–58.

35. Yu JM, Kim JH, Song GS, Jung JS. Increase in proliferation and differentiation of neural progenitor cells isolated from postnatal and adult mice brain by Wnt-3a and Wnt-5a. *Mol Cell Biochem* 2006;288:17–28.

36. Wick W, Plattan M, Weller M. New (alternative) temozolomide regimens for the treatment of glioma. *Neuro Oncol* 2009;11:69–79.

37. Katoh M, Katoh M. WNT signalling pathway and stem cells signaling network. *Clin Cancer Res* 2007;13:4042–45.

38. MacDonald BT, Tamai K, He X. Wnt/β-catenin signaling: components, mechanisms, and diseases. *Dev Cell* 2009;17:9–26.

39. Flahaut M, Meier R, Coulon A, et al. The Wnt receptor FZD1 mediates chemoresistance in neuroblastoma through activation of the Wnt/b-catenin pathway. *Oncogene* 2009;28:2245–2256.

40. Bexell D, Gunnarsson S, Siesj P, Bengzon J, Darabi A. CD133+ and nestin+ tumor-initiating cells dominate in N29 and N32 experimental gliomas. *Int J Cancer* 2009;125:15–22.

41. Gilbert CA, Daou MC, Moser RP, Ross AH. Gamma-Secretase Inhibitors Enhance Temozolomide Treatment of Human Gliomas by Inhibiting Neurosphere Repopulation and Xenograft Recurrence. *Cancer Res* 2010;70: 6870–6879.

42. Sankar A, Thomas DG, Darling JL. Sensitivity of short-term cultures derived from human malignant glioma to the anti-cancer drug temozolomide. *Anticancer Drugs* 1999;10:179−85.

43. Zheng H, Ying H, Wiedemeyer R, et al. PLAGL2 Regulates Wnt Signaling to Impede Differentiation in neural stem cells and gliomas. *Cancer Cell* 2010;17:497–509.

44. Zhang N, Wei P, Gong A, et al. FoxM1 promotes β-catenin nuclear localization and controls Wnt target Expression and glioma tumorigenesis. Cancer Cell 2011;20:427–442.

45. Shou J, Ali-Osman F, Multani AS, Pathak S, Fedi P, Srivenugopal KS. Human Dkk-1, a gene encoding a Wnt antagonist, responds to DNA damage and its overexpression sensitize. *Oncogene* 2002;21:878–889.

46. Kobune M, Chiba H, Kato J, et al. Wnt3/RhoA/ROCK signaling pathway is involved in adhesion-mediated drug resistance of multiple myeloma in an autocrine mechanism. *Mol Cancer Ther* 2007;6:1774–1784.

Figure captions

Fig. 1. Characterization of NS and AC GBM cells.

(A) Morphologic analysis of CV17, 010627 and U87-MG GBM cells, cultured as neurospheres (*NS*) or adherent cells (*AC*), and analyzed by a bright field microscope. Magnification: 100 x objective (0.52 numerical aperture); 10 x ocular lens. Bar: 20 μm. (B) Clonogenic assay. Neurospheres (*NS*) or adherent cells (*AC*) were seeded at a density of 100 cells/well; the number of spheres or adherent colonies was counted at day 14, 28, 42. Data are

presented as means ± SD (n=6). Significance of *NS* vs *AC*: * $p < 0.01$. (C) Self-renewal assay. Neurospheres (*NS*) or adherent cells (*AC*) were diluted and seeded at a density of 1 cell/well; the number of cells was counted at day 14, 28, 42. Data are presented as means ± SD (n=10). Since AC had a value of 1 cell ± 0 at each time point, the statistic analysis was not performed. (D) Cell cycle analysis. The distribution of neurospheres (*NS*) or adherent cells (*AC*) in sub-G1, G0/G1, S, G2/M phase was analyzed by flow cytometry, as detailed under Materials and methods. Data are presented as means ± SD (n=4). Significance of *NS* vs *AC*: * $p < 0.05$.

Fig. 2. Effects of TMZ and doxorubicin on GBM cells.

(A-C) Drug-induced cell damages. Neurospheres (*open columns, NS*) and adherent cells (*hatched columns, AC*) were incubated for 72 h with fresh medium (-) or TMZ at 50, 100, 200 μM (*T*; panel A), 5 μM doxorubicin for 24 h (*dox*; panel B) or with 50 μM TMZ for 72 h plus 5 μM doxorubicin for the last 24 h (panel C). The human doxorubicin-sensitive colon cancer HT29 cells and the doxorubicin-resistant counterpart HT29-dx cells were used in Fig. 2B as positive controls of drug-sensitive and drug-resistant cells, respectively. The culture medium was collected and analyzed in duplicate for the LDH release, as index of cytotoxicity. Data are presented as means ± SD (n=4). Significance vs untreated (-) cells: * $p < 0.02$; *T* + *dox* vs *T* alone: ° $p < 0.05$. (D) NS were seeded at a concentration of 100 cells/well, left untreated (*ctrl*) or treated at day 4, 11, 18, 25, 32, 39 with 50 μM TMZ (*T*) for 72 h, 5 μM doxorubicin for 24 h, or TMZ for 72 h with the addition of doxorubicin in the last 24 h. At the end of each treatment, cells were washed and re-seeded in fresh medium. The spheres formed in each well were counted at day 14, 28 and 42. Data are presented as means ± SD (n=4). Significance vs untreated cells: * $p < 0.02$; *T* + *dox* vs *T* alone: ° $p < 0.005$. (E) NS incubated as reported in (C) were subjected to the cell cycle analysis. Data are presented

as means ± SD (n=3). Significance vs untreated (-) cells: * $p < 0.01$; *T* + *dox* vs *T* alone: ° $p < 0.02$.

Fig. 3. Effects of TMZ, vinblastine and etoposide on NS GBM cells.

(A) Drug-induced cell damages. NS were incubated with fresh medium (-) or 50 μM TMZ for 72 h (*T*), 20 nM vinblastine for 24 h (*VBL*), 10 μM etoposide for 24 h (*ETO*), or with 50 μM TMZ for 72 h with the addition of vinblastine or etoposide in the last 24 h. The culture medium was collected and analyzed in duplicate for the LDH release, as index of cytotoxicity. Data are presented as means ± SD (n=3). Significance vs untreated (-) cells: * $p < 0.05$; *T* + *VBL/ETO* vs *T* alone: ° $p < 0.05$. (B) NS were seeded in the plate at a concentration of 100 cells/well, left untreated (*ctrl*) or treated at day 4, 11, 18, 25, 32, 39 with 50 μM TMZ (*T*) for 72 h, 20 nM vinblastine for 24 h (*VBL*), 10 μM etoposide for 24 h (*ETO*), or with 50 μM TMZ for 72 h plus vinblastine or etoposide in the last 24 h. At the end of each treatment, cells were washed and re-seeded in fresh medium. The spheres formed in each well were counted at day 14, 28 and 42. Data are presented as means ± SD (n=4). Significance vs untreated cells: * $p < 0.05$; *T* + *VBL/ETO* vs *T* alone: ° $p < 0.001$. (C) NS incubated as reported in (A) were subjected to the cell cycle analysis. Data are presented as means ± SD (n=3). Significance vs untreated (-) cells: * $p < 0.05$; *T* + *dox* vs *T* alone: ° $p < 0.05$.

Fig. 4. Expression levels of *Wnts* and *ABCB1* genes in GBM cells.

CV17, 010627 and U87-MG GBM cells, cultured as adherent cells (*open columns*, *AC*) or neurospheres (*hatched columns, NS*), were subjected to RNA extraction and qRT-PCR to measure the expression of *Wnt3a*, *Wnt5* (*Wn*, panel A) and *ABCB1* (panel B). The expression level of CV17 *AC* was considered "1" and used as reference for all the other experimental

conditions. Data are presented as means ± SD (n = 3). Vs CTRL: * $p < 0.05$. (C) Time-dependent expression of *Wnt3a* and *ABCB1* gene in CV17, 010627 and U87-MG neurospheres (*NS*), incubated in the absence (-) or presence of 50 μM TMZ (*T*) for 24, 48, 72 h. The expression level of CV17 cells was considered "1" and used as reference for all the other experimental conditions. Data are presented as means ± SD (n = 3). Vs CTRL: * $p < 0.05$. (D) Methylation of *Wnt3a* promoter. Genomic DNA from CV17, 010627, U87-MG, No3 NS, incubated in fresh medium (-) or with 50 μM TMZ (*T*) for 48 h was subjected to bisulfite modification, followed by PCR with specific primers for methylated (*M*) and unmethylated (*UM*) *Wnt3a* promoter. The figure is representative of 3 experiments with similar results. +: positive controls with a universally methylated or unmethylated genome sequence. *bl*: blank.

Fig. 5. Effects of Wnt3a overexpression and silencing on morphology and proliferation in 010627 GBM cells.

(A) Adherent (*AC*) 010627 cells (*grey peak*) were transfected with a pCMV6-AC-GFP empty vector (*dotted line*) or with Wnt3a-pCMV6-AC-GFP expression vector (*$Wnt3a^+$; continuous line*). Neurospheres (*NS*) 010627 cells (*grey peak*) were transfected with a 29-mer scrambled shRNA pGFP-V-RS vector (*dotted line*) or with a pGFP-V-RS shRNA-Wnt3a vector (*$Wnt3a^-$; continuous line*). The efficiency of transfection was checked by flow cytometry after 24 h. The figures shown here are representative of 3 similar experiments, each performed in triplicate. (B) *Wnt3a* expression was detected 48 h after the transfection in triplicate by qRT-PCR. The expression level of 010627 AC was considered "1" and used as reference for all the other experimental conditions. Data are presented as means ± SD (n = 3). Vs 010627 *AC* ctrl: * $p < 0.02$; vs 010627 *NS* ctrl: ° $p < 0.001$. (C) Microscope analysis of the Wnt3a overexpressing adherent 010627 cells (*010627 AC $Wnt3a^+$*) and of Wnt3a silenced 010627

neurospheres (*010627 NS Wnt3a* $^{-}$). The samples were analyzed by Nomarski differential interference contrast optics (*DIC; left panel*) or by FV300 laser scanning confocal microscope for green fluorescence protein signal (*GFP; right panel*). The micrographs are representative of the cell morphology 72 h after the transfection. Magnification: 60 x objective (1.4 numerical aperture); 10 x ocular lens. (D) Cell proliferation was measured in triplicate 96 h after the transfection by the [^{3}H]-thymidine incorporation assay. Data are presented as means $\pm$ SD (n = 3). Vs 010627 *AC* ctrl: ***** $p < 0.001$; vs 010627 *NS* ctrl: **°** $p < 0.001$. (E) Clonogenic assay. Wild-type AC 010627 cells (*ctrl*), AC 010627 cells transfected with a pCMV6-AC-GFP empty vector (*empty*), AC 010627 cells stably overexpressing Wnt3a (*Wnt3a*$^{+}$), wild-type NS 010627 cells (*ctrl*), NS 010627 transfected with a 29-mer scrambled shRNA pGFP-V-RS vector (*scrambled*), NS 010627 stably silenced for Wnt3a (*Wnt3a* $^{-}$) were seeded at a density of 100 cells/well; the number of spheres or adherent colonies was counted at day 14, 28, 48. Data are presented as means $\pm$ SD (n=4). Significance of *Wnt3a*$^{+}$ or *Wnt3a*$^{-}$ vs the respective *ctrl*: ***** $p < 0.002$. (C) Self-renewal assay. *NS* or *AC* were diluted and seeded at a density of 1 cell/well; the number of cells was counted at day 14, 28, 48. Data are presented as means $\pm$ SD (n=10). Since wild-type AC 010627 cells and AC 010627 cells transfected with the empty vector had a value of 1 cell $\pm$ 0 at each time point, the statistic analysis was not performed.

Fig. 6. Effects of Wnt3a overexpression and silencing on GSK3/β-catenin pathway and *ABCB1* expression in 010627 GBM cells.

Adherent (*AC*) 010627 cells were transfected with a pCMV6-AC-GFP empty vector (*empty*) or with Wnt3a-pCMV6-AC-GFP expression vector (*Wnt3a*$^{+}$). Neurospheres (*NS*) 010627 cells were transfected with a 29-mer scrambled shRNA pGFP-V-RS vector (*scrambled*) or with a pGFP-V-RS shRNA-Wnt3a vector (*Wnt3a* $^{-}$). (A) Western blot analysis (96 h after the

transfection) of GSK3, phospho(Tyr216)GSK3 (*p-GSK3*), β-catenin, phospho(Ser33/37/Thr41)β-catenin (*p-catenin*) in whole cell lysates. Tubulin expression was used as control of equal protein loading. The figure is representative of 3 experiments with similar results. (B) *ABCB1* expression was detected in triplicate by qRT-PCR 96 h after the transfection. The expression level of 010627 AC was considered "1" and used as reference for all the other experimental conditions. Data are presented as means ± SD (n = 3). Vs 010627 *AC* ctrl: * $p < 0.01$; vs 010627 *NS* ctrl: ° $p < 0.001$.

Fig 7. Effects of TMZ on Wnt3a/GSK3/β-catenin/Pgp axis in GBM cells.

CV17, 010627 and U87-MG GBM cells, cultured as adherent cells (*AC*) or neurospheres (*NS*), were incubated for 48 h in the absence (-) or presence (+) of 50 μM TMZ.
(A) Western blot analysis of Wnt3a, GSK3, phospho(Tyr216)GSK3 (*p-GSK3*), β-catenin, phospho(Ser33/37/Thr41)β-catenin (*p-catenin*) in whole cell lysates. Tubulin expression was used as control of equal protein loading. The figure is representative of 3 experiments with similar results. (B) Nuclear and cytosolic extracts prepared from neurospheres (*NS*) were analyzed for the amount of β-catenin. The expression of tubulin and TBP were used as control of equal protein loading for cytosolic and nuclear samples, respectively. The figure is representative of 2 experiments with similar results. (C) Chromatin immunoprecipitation of β-catenin on *ABCB1* promoter in 010627 *NS* cells. *no Ab*: precipitated samples without anti-β-catenin antibody. *bl*: blank. The figure is representative of 3 experiments with similar results.

Fig. 8. Effects of TMZ on Pgp expression and activity in GBM cells.

(A) CV17, 010627 and U87-MG GBM cells, cultured as neurospheres (NS), were incubated for 72 h in the absence (-) or presence (+) of 50 μM TMZ. Cells were lysed and subjected to

Western blot for Pgp protein. Tubulin expression was used as control of equal protein loading. The figure is representative of 2 experiments with similar results. (B) NS were grown in fresh medium (*CTRL*), with 10 μM verapamil (*VER*) or cyclosporine A (*CSA*) for 24 h, or 50 μM TMZ for 72 h, then incubated with the Pgp substrate rhodamine 123. The activity of Pgp, measured as the rate of efflux of rhodamine, was evaluated by flow cytometry (see Materials and Methods). The figures shown here are representative of three similar experiments, performed in duplicate. (C) NS were incubated for 24 h in fresh medium (-), or in the presence of 5 μM doxorubicin (*dox*), 20 nM vinblastine (*VBL*), 10 μM etoposide (*ETO*), alone (*no Pgp inhibitors*) or together with 10 μM verapamil (*VER*) or 10 μM cyclosporine A (*CSA*). The culture medium was collected and analyzed in duplicate for the LDH release, as index of cytotoxicity. Data are presented as means $\pm$ SD (n=3). Significance vs untreated (-) cells: ***** $p < 0.01$; *dox/VBL/ETO+VER* or *CSA* vs *dox/VBL/ETO* alone: ° $p < 0.01$.

Supplementary Figures captions

Supplementary Fig. 1. *In vivo* tumorigenicity.

Histological analysis of FFPE brains after intracranial transplantation of CV17 AC (*A*) or NS (*B*). The images are from one representative of 4 mice per each group.

Supplementary Fig. 2. Expression of O^6-methylguanine-DNA methyltransferase (MGMT) in GBM cells.

CV17, 010627 and U87-MG GBM cells, cultured as neurospheres (*NS*) or adherent cells (*AC*), were lysed and subjected to Western blot for MGMT protein. Tubulin expression was used as control of equal protein loading. The figure is representative of 3 experiments with similar results.

Supplementary Fig. 3. Effects of TMZ and cisplatin on NS GBM cells.

(A) Drug-induced cell damages. NS were incubated with fresh medium (-) or 50 μM TMZ for 72 h (*T*), 10 μM cisplatin for 24 h (*Pt*), or with 50 μM TMZ for 72 h with further addition of cisplatin in the last 24 h. The culture medium was collected and analyzed in duplicate for the LDH release, as index of cytotoxicity. Data are presented as means $\pm$ SD (n=3). (B) NS were seeded at a concentration of 100 cells/well, left untreated (*ctrl*) or treated at day 4, 11, 18, 25, 32, 39 with 50 μM TMZ for 72 h, 10 μM cisplatin for 24 h, or with 50 μM TMZ for 72 h with further addition of cisplatin in the last 24 h. At the end of each treatment, cells were washed and re-seeded in fresh medium. The spheres formed in each well were counted at day 14, 28 and 42. Data are presented as means $\pm$ SD (n=4). (C) NS incubated as reported in (A) were subjected to the cell cycle analysis. Data are presented as means $\pm$ SD (n=3). Significance vs untreated (-) cells: ***** $p < 0.01$.

Supplementary Fig. 4. Effects of TMZ and methotrexate on NS GBM cells.

(A) Drug-induced cell damages. NS were incubated with fresh medium (-) or 50 μM TMZ for 72 h (*T*), 2 μM methotrexate for 24 h (*MTX*), or with 50 μM TMZ for 72 h with further addition of methotrexate in the last 24 h. The culture medium was collected and analyzed in duplicate for the LDH release, as index of cytotoxicity. Data are presented as means ± SD (n=3). (B) NS were seeded at a concentration of 100 cells/well, left untreated (*ctrl*) or treated at day 4, 11, 18, 25, 32, 39 with 50 μM TMZ for 72 h, 2 μM methotrexate for 24 h, or with 50 μM TMZ for 72 h with further addition of methotrexate in the last 24 h. At the end of each treatment, cells were washed and re-seeded in fresh medium. The spheres formed in each well were counted at day 14, 28 and 42. Data are presented as means ± SD (n=4). (C) NS incubated as reported in (A) were subjected to the cell cycle analysis. Data are presented as means ± SD (n=3). Significance vs untreated (-) cells: * $p < 0.01$.

Supplementary Fig. 5. Effects of TMZ and mitoxantrone on NS GBM cells.

(A) Drug-induced cell damages. NS were incubated with fresh medium (-) or 50 μM TMZ for 72 h (*T*), 5 μM mitoxantrone for 24 h (*MXR*), or with 50 μM TMZ for 72 h with further addition of mitoxantrone in the last 24 h. The culture medium was collected and analyzed in duplicate for the LDH release, as index of cytotoxicity. Data are presented as means ± SD (n=3). (B) NS were seeded at a concentration of 100 cells/well, left untreated (*ctrl*) or treated at day 4, 11, 18, 25, 32, 39 with 50 μM TMZ for 72 h, 5 μM mitoxantrone for 24 h, or with 50 μM TMZ for 72 h with further addition of mitoxantrone in the last 24 h. At the end of each treatment, cells were washed and re-seeded in fresh medium. The spheres formed in each well were counted at day 14, 28 and 42. Data are presented as means ± SD (n=4). (C)

NS incubated as reported in (A) were subjected to the cell cycle analysis. Data are presented as means ± SD (n=3). Significance vs untreated (-) cells: * $p < 0.01$.

Supplementary Fig. 6. Expression of *Notch1, Notch2, Notch3, Notch4, Sonic Hedgehog* in GBM cells.

CV17, 010627 and U87-MG GBM cells, grown as adherent cells (*AC; open columns*) or neurospheres (*NS; hatched columns*), were subjected to RNA extraction and qRT-PCR to measure the expression of *Notch1*, *Notch2*, *Notch3*, *Notch4* (*Not*; panel A)*, Sonic Hedgehog* (*SHH;* panel B). The expression level of CV17 AC was considered "1" and used as reference for all the other experimental conditions. Data are presented as means ± SD (n = 3). Vs CTRL: * $p < 0.05$.

Supplementary Fig. 7. Expression of *ABCC1* and *ABCG2* gene in GBM cells.

(A-B) CV17, 010627 and U87-MG, grown as adherent cells (*AC; open columns*) or neurospheres (*NS; hatched columns*), were checked for the basal expression of *ABCC1* (panel A) and *ABCG2* (panel B) genes by qRT-PCR. The expression level of CV17 AC was considered "1" and used as reference for all the other experimental conditions. Data are presented as means ± SD (n = 3). Significance vs *AC* cells: * $p < 0.05$. (C) NS were incubated in the absence (-) or presence of 50 μM TMZ (*T*) for 24, 48, 72 h; the expression of *ABCC1* (*open bars*) and *ABCG2* (*hatched bars*) was measured by qRT-PCR. The expression level of CV17 cells was considered "1" and used as reference for all the other experimental conditions. Data are presented as means ± SD (n = 2).

Supplementary Fig. 8. Localization of CpG islands on the promoter of *Wnt3a* and *ABCB1* genes.

CpG islands localization on *Wnt3a* promoter (panel A) and *ABCB1* promoter (panel B), according to Methprimer software (http://www.urogene.org/methprimer), using as input the promoter sequence obtained by the UCSC Genome Browser (http://genome.ucsc.edu/).

Supplementary Fig. 9. Presence of 5 methyl cytosines (5mC) in the promoter of *Wnt3a* after TMZ and 5-aza-2'-deoxycytidine treatment.

010627 NS were incubated for 24 h in fresh medium (*CTRL*), with 50 μM TMZ, 100 μM 5-aza-2'-deoxycytidine (*AZA*), an agent that inhibits the methylation of cytosine on position 5 by DNA methyltransferases, alone or in combination. Genomic DNA was extracted and subjected to the PCR amplification of the CpG islands-rich fragment of the *Wnt3a* promoter. (A) Immunoprecipitation (IP) of DNA containing 5mC. 100 ng of the PCR product were immunoprecipitated with 1 μg of an anti-5mC antibody, then resolved on agarose gel (*prom Wnt3a*). *no Ab*: precipitated samples without anti-5mC antibody. *bl*: blank. *Gen prom Wnt3a*: PCR product from the genomic DNA. The figure is representative of 3 experiments with similar results. (B) ELISA quantification of 5mC. The amount of 5mC present in the CpG islands-rich fragment of the *Wnt3a* promoter was measured in triplicate, as reported under Materials and Methods. Data are presented as means ± SD (n = 3). Vs CTRL: * $p < 0.005$; vs TMZ: ° $p < 0.005$.

Supplementary Fig. 10. Effects of BCNU on *Wnt3a* and *ABCB1* expression and LDH release in GBM cells.

CV17, 010627 and U87-MG neurospheres (*NS*) were incubated for 168 h in the absence (-) or presence (*BC*) of 50 μM BCNU.

(A) Total RNA was extracted and reverse-transcribed, then the expression of *Wnt3a* (*open columns*) and *ABCB1* (*hatched columns*) genes was detected by qRT-PCR. The expression

level of CV17 cells was considered "1" and used as reference for all the other experimental conditions. Data are presented as means ± SD (n = 3). (B) The medium of cultures was collected and analyzed in duplicate for the LDH release, as index of cytotoxicity. Data are presented as means ± SD (n = 4). Significance vs untreated cells: * $p < 0.001$.

Supplementary Fig. 11. Morphologic analysis and *Wnt3a/ABCB1* expression in stably 010627 AC Wnt3a$^+$ cells and 010627 NS Wnt3a$^-$ cells.

(A) Wild-type non transfected *010627 AC* and *010627 NS* cells; *010627 AC Wnt3a*$^+$ cells at day 1, at passage 10 and at passage 20 after the transfection; *010627 NS Wnt3a*$^-$ cells at day 1, at passage 10 and at passage 20 after the transfection, were seeded (if AC) or cyto-spun (if NS) on glass coverslips, stained with DAPI and analyzed by fluorescence microscope. The figures are representative of two similar experiments. Magnification: 63 x objective (1.4 numerical aperture); 10 x ocular lens. (B-C) Wild-type (*wt*) non transfected *010627 AC* and *010627 NS* cells, stably *010627 AC Wnt3a*$^+$ cells (collected at passage 10 and 20) and stably *010627 NS Wnt3a*$^-$ cells (collected at passage 10 and 20) were checked by qRT-PCR for the expression of *Wnt3a* (panel B) and *ABCB1* (panel C) genes. The expression level of 010627 AC was considered "1" and used as reference for all the other experimental conditions. Data are presented as means ± SD (n = 3). Significance vs 010627 *AC wt*: * $p < 0.01$; vs 010627 *NS wt*: ° $p < 0.02$.

Supplementary Fig. 12. Effects of TMZ on the expression of Frizzled and LRP receptors in GBM cells.

CV17, 010627 and U87-MG GBM cells, grown as adherent cells (*AC*) or neurospheres (*NS*), were incubated for 48 h in fresh medium (*CTRL*) or with 50 μM TMZ. Flow cytometry analysis of surface Frizzled (panel A) and LRP6 (panel B). *Grey peak*: cells treated with anti-

isotypic antibody (*blank*). The figures shown here are representative of 3 similar experiments, each performed in triplicate.

Supplementary Fig. 13. Effects of Wnt3a-signalling modulators on *ABCB1* expression in GBM cells.

010627 *NS* cells were incubated with fresh medium (*CTRL*), TMZ (50 μM for 48 h), the Wnt activator 2-amino-4-(3,4-(methylenedioxy)benzylamino)-6-(3-methoxyphenyl)pyrimidine (*WntA*; 20 μM for 24 h), the Wnt inhibitor recombinant DKK-1 protein (*DKK*; 1 μg/ml for 24 h); the GSK3 inhibitor LiCl (*LiCl*; 10 mM for 24 h), alone or in different combinations. *ABCB1* expression was detected in triplicate by qRT-PCR. Data are presented as means $\pm$ SD (n = 4). Vs CTRL: * $p < 0.02$; vs WntA or LiCl: ° $p < 0.05$.

Supplementary Tables

Supplementary Table 1. Primers sequences of quantitative Real Time-PCR (qRT-PCR), immunoprecipitation (IP), ELISA, methylation specific PCR (MSP) and chromatin immunoprecipitation (ChIP)

Gene	Assay	Forward primer (5'-3')	Reverse primer (5'-3')
Wnt3a	qRT-PCR	TGTGCTAAAGACAGCTTG'	GGAGATGCGTTGAACTCTC
Wnt5	qRT-PCR	CCACATGCAGTACATCGGAG	TGCCGGAAGTGTATGCG
Notch1	qRT-PCR	TCAGCGGGATCCACTGTGAG	ACACAGGCAGGTGAGTTC
Notch2	qRT-PCR	ATGCTCAGCCGGGATACCT	GGTTGGCCACAGTGGTACAGG
Notch3	qRT-PCR	AAGGACGTGGCCTCTGGT	TCAGGCTCTCACCCTTGG
Notch4	qRT-PCR	TGAGGTGAATCCAGACAAC	ATACAGTCATCCAGGTTCTC
SHH	qRT-PCR	CGGCTTCGACTGGGTGTACT	GCAGCCTCCCGATTTGG
ABCB1	qRT-PCR	TGCTGGAGCGGTTCTACG	ATAGGCAATGTTCTCAGCAATG
ABCC1	qRT-PCR	CATTCAGCTCGTCTTGTCCTG	GGATTAGGGTCGTGGATGGTT
ABCG2	qRT-PCR	GTTTCAGCCGTGGAAC	CTGCCTTTGGCTTCAAT
β-actin	qRT-PCR	GCTATCCAGGCTGTGCTATC	TGTCACGCACGATTTCC
Wnt3a promoter	IP, ELISA	CACAGACCAGGAGCGAGAG	GCTCCGAGCTGTTCAGTCTT
Wnt3a promoter (methylated)	MSP	TTAGTTATTTCGGGGGTAAGAGAC	CCAAATAAACAAACGACCGA
Wnt3a promoter (unmethylated)	MSP	TTTAGTTATTTTGGGGGTAAGAGAT	CAAATAAACAAACAACCAAC
ABCB1 (promoter)	ChIP	CGATCCGCCTAAGAACAAAG	AGCACAAATTGAAGGAAGGAG
ABCB1 (upstream sequence)	ChIP	GTGGTGCCTGAGGAAGAGAG	GCAACAAGTAGGCACAAGCA
ABCB1 (genomic)	ChIP	GACCAAGCTCTCCTTGCATC	AGGGAAGTCTGGCAGCTGTA

Supplementary Table 2. Phenotypic characterization of CV17, 010627 and U87-MG cells by immunofluorescence analysis.

Marker	NS CV17	NS 010627	NS U87	AC CV17	AC 010627	AC U87
Nestin	++	+	+	+	+	+
CD133	-	+	-	+	-	-
Musashi	-	+	-	+	-	-
SOX2	+	+	+	-	-	-
EGFR	+/-	+	+	+	-	-
p53	+	+	-	-	-	-
GFAP	-	-	-	+	+	+
GalC	+	-	-	+	+/-	+/-

Figure 1

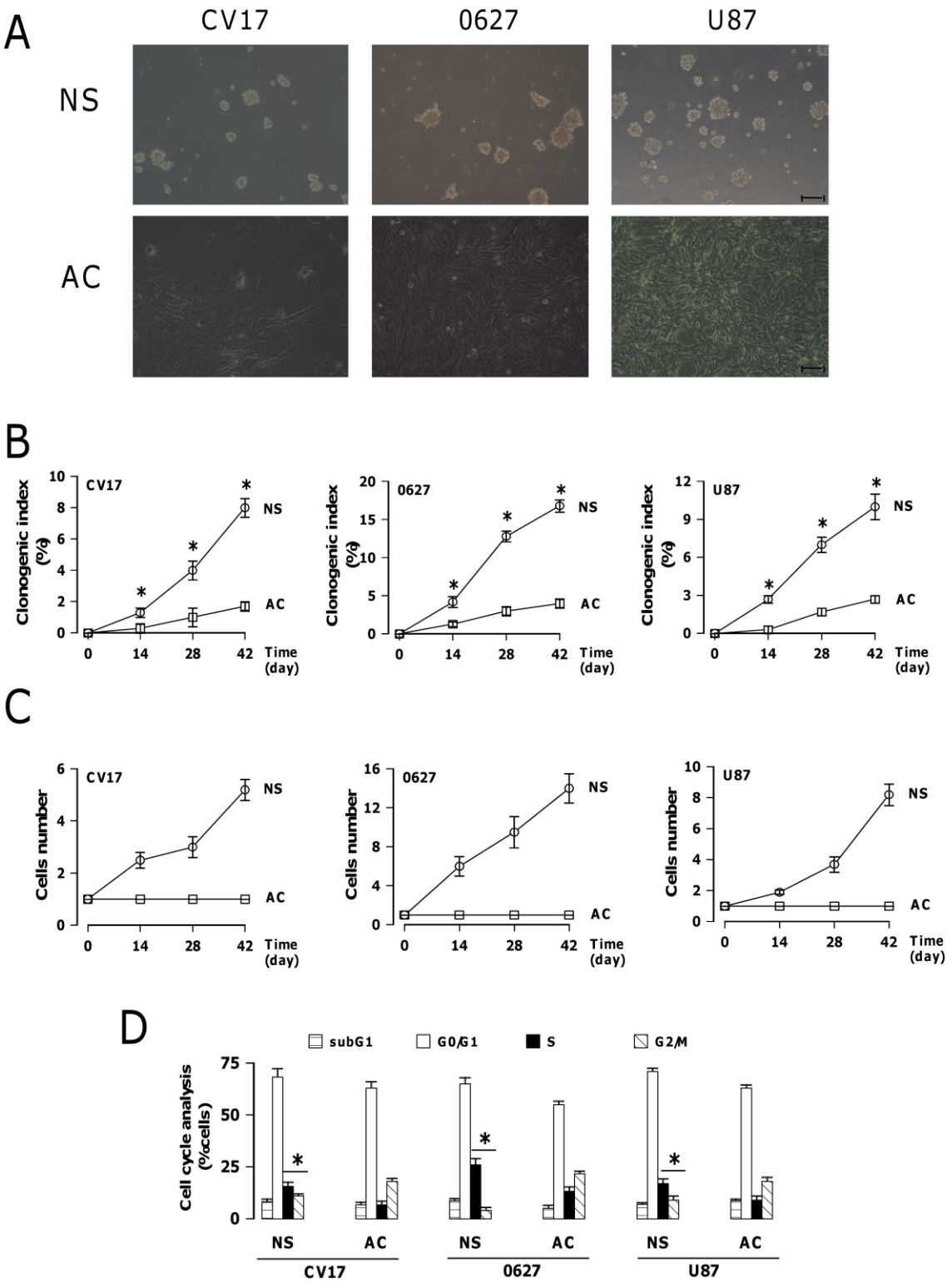
A
CV17
0627
U87
NS
AC
B
Clonogenic index (%)
CV17
0627
U87
NS
AC
Time (day)
C
Cells number
CV17
0627
U87
NS
AC
Time (day)
D
subG1
G0/G1
S
G2/M
Cell cycle analysis (%cells)
NS
AC
CV17
0627
U87

Figure 2

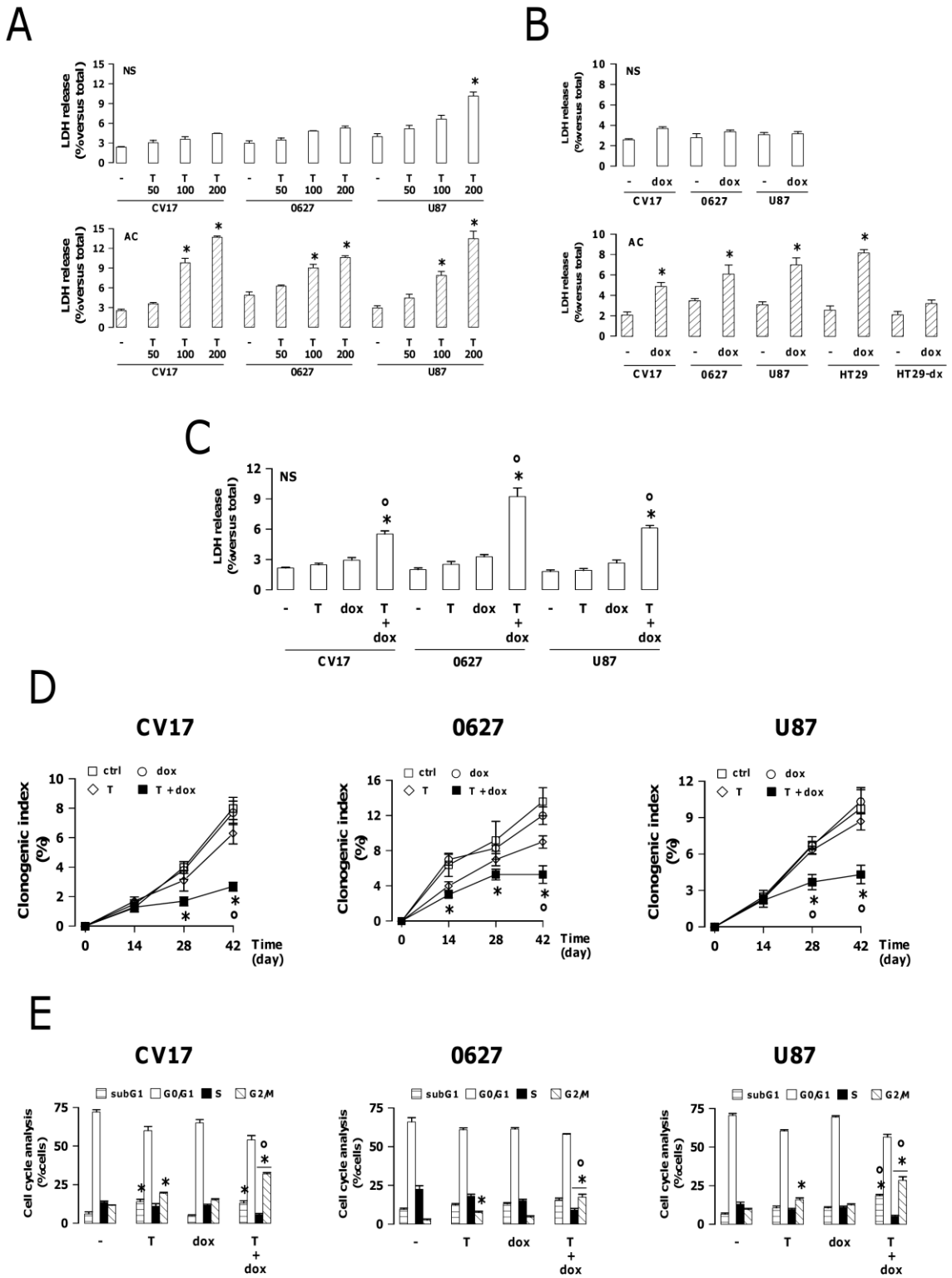
A
NS
AC
LDH release (%versus total)
- T 50 T 100 T 200
CV17
0627
U87
B
NS
AC
- dox
CV17
0627
U87
HT29
HT29-dx
C
NS
- T dox T + dox
CV17
0627
U87
D
CV17
0627
U87
ctrl
dox
T
T +dox
Clonogenic index (%)
Time (day)
E
CV17
0627
U87
subG1
G0/G1
S
G2/M
Cell cycle analysis (%cells)
- T dox T + dox

Figure 3

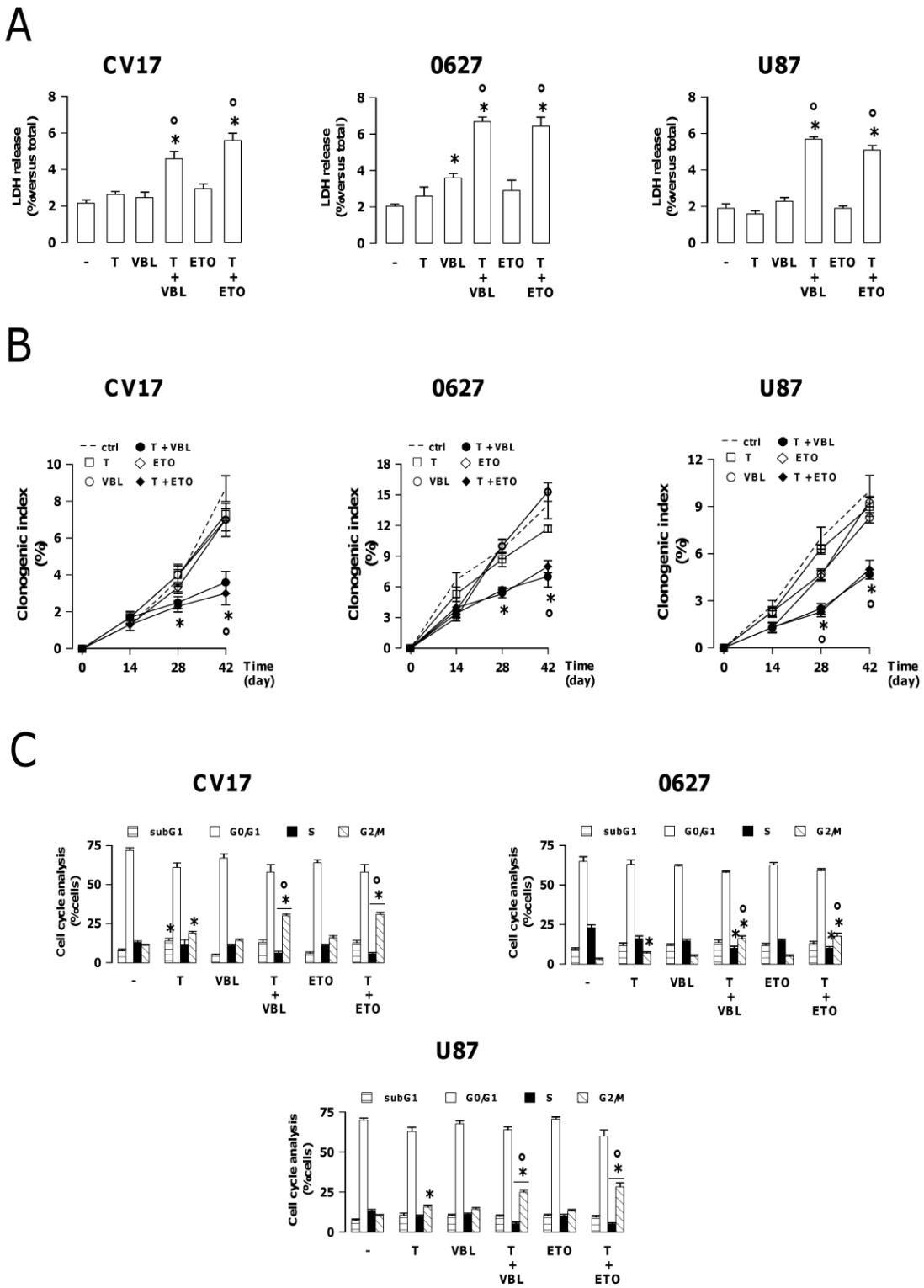
A
CV17
0627
U87
LDH release (%versus total)
- T VBL T + VBL ETO T + ETO
B
CV17
0627
U87
ctrl
T
VBL
T +VBL
ETO
T +ETO
Clonogenic index (%)
Time (day)
C
CV17
0627
U87
subG1
G0/G1
S
G2/M
Cell cycle analysis (%cells)

Figure 4

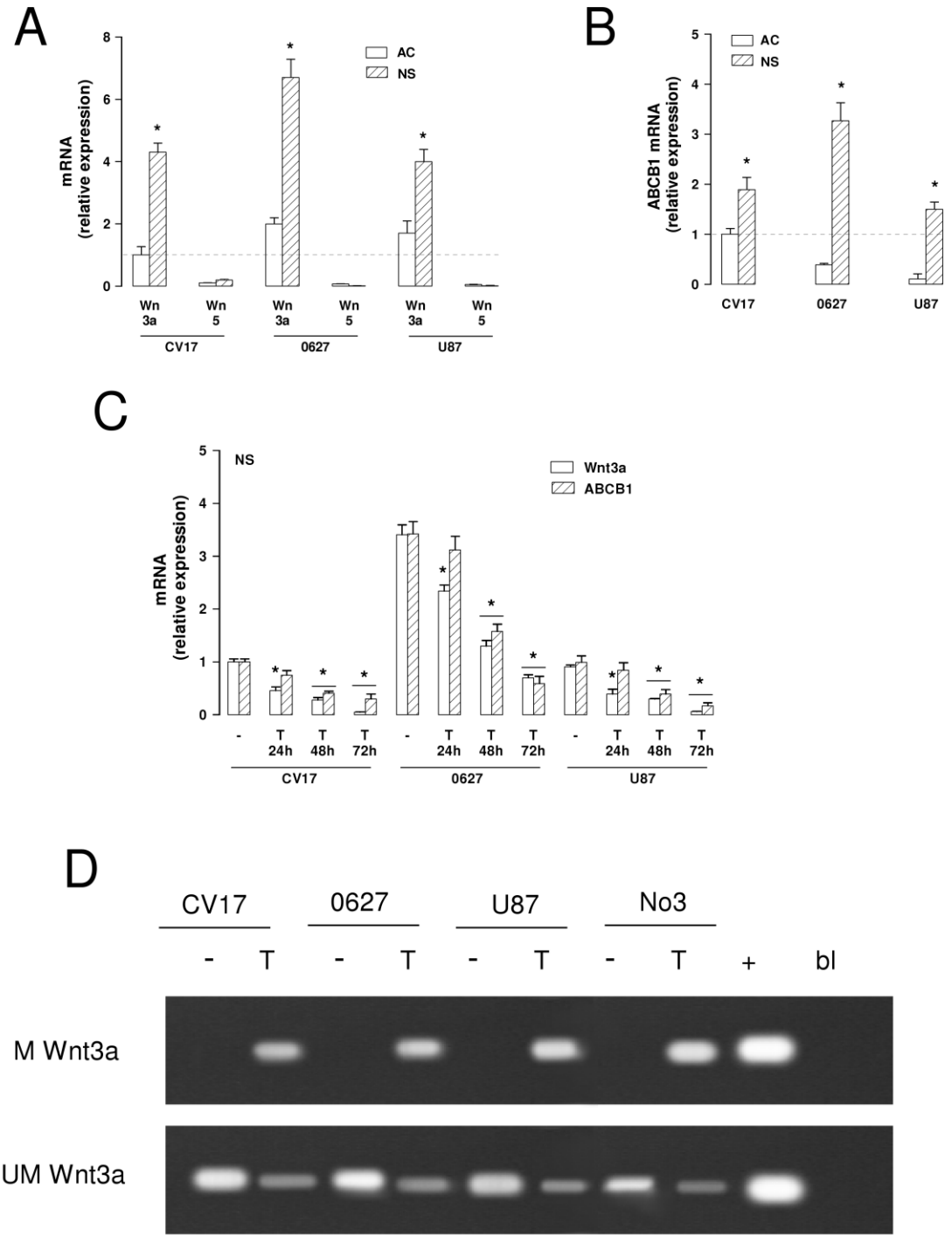
A
mRNA (relative expression)
AC
NS
Wn 3a
Wn 5
CV17
0627
U87
B
ABCB1 mRNA (relative expression)
AC
NS
CV17
0627
U87
C
NS
Wnt3a
ABCB1
mRNA (relative expression)
-
T 24h
T 48h
T 72h
CV17
0627
U87
D
CV17
0627
U87
No3
- T - T - T - T + bl
M Wnt3a
UM Wnt3a

Figure 5

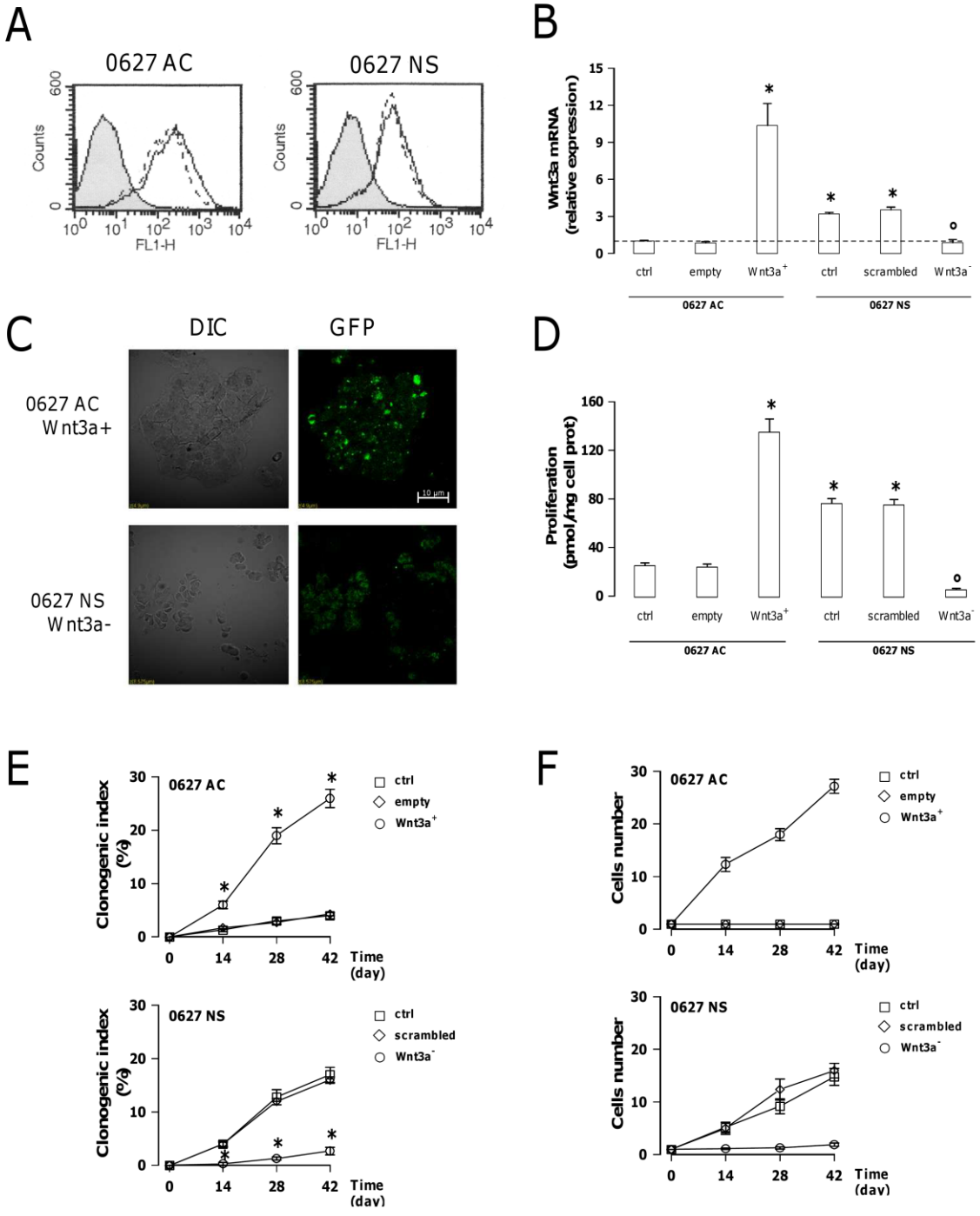
A
0627 AC
0627 NS
Counts
FL1-H
B
Wnt3a mRNA (relative expression)
ctrl
empty
Wnt3a+
scrambled
Wnt3a-
0627 AC
0627 NS
C
DIC
GFP
0627 AC Wnt3a+
0627 NS Wnt3a-
10 µm
D
Proliferation (pmol/mg cell prot)
E
Clonogenic index (%)
Time (day)
F
Cells number

Figure 6

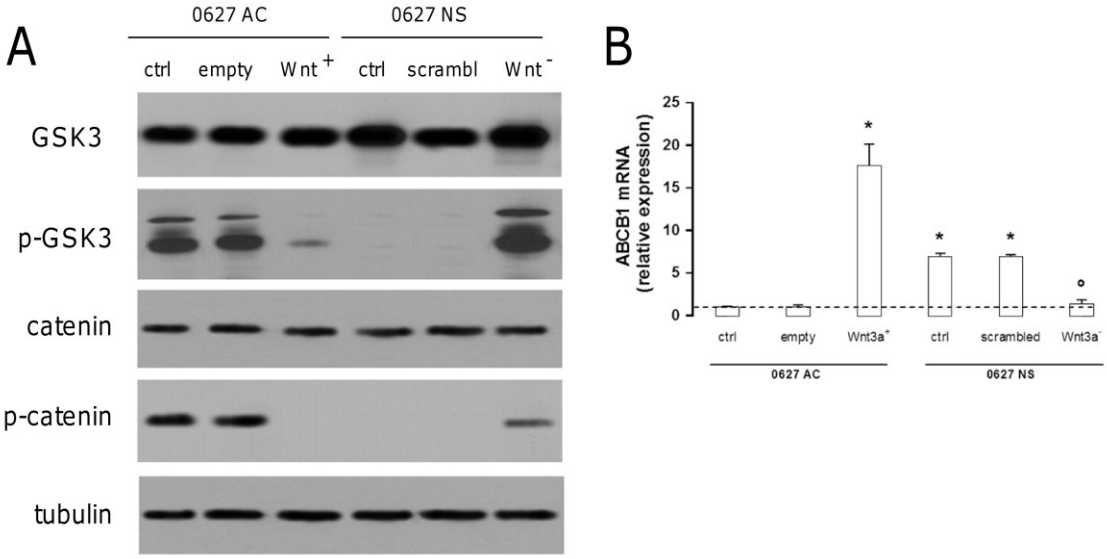
A
0627 AC
0627 NS
ctrl
empty
Wnt+
ctrl
scrambl
Wnt-
GSK3
p-GSK3
catenin
p-catenin
tubulin
B
ABCB1 mRNA
(relative expression)
25
20
15
10
5
0
ctrl
empty
Wnt3a+
ctrl
scrambled
Wnt3a-
0627 AC
0627 NS

Figure 7

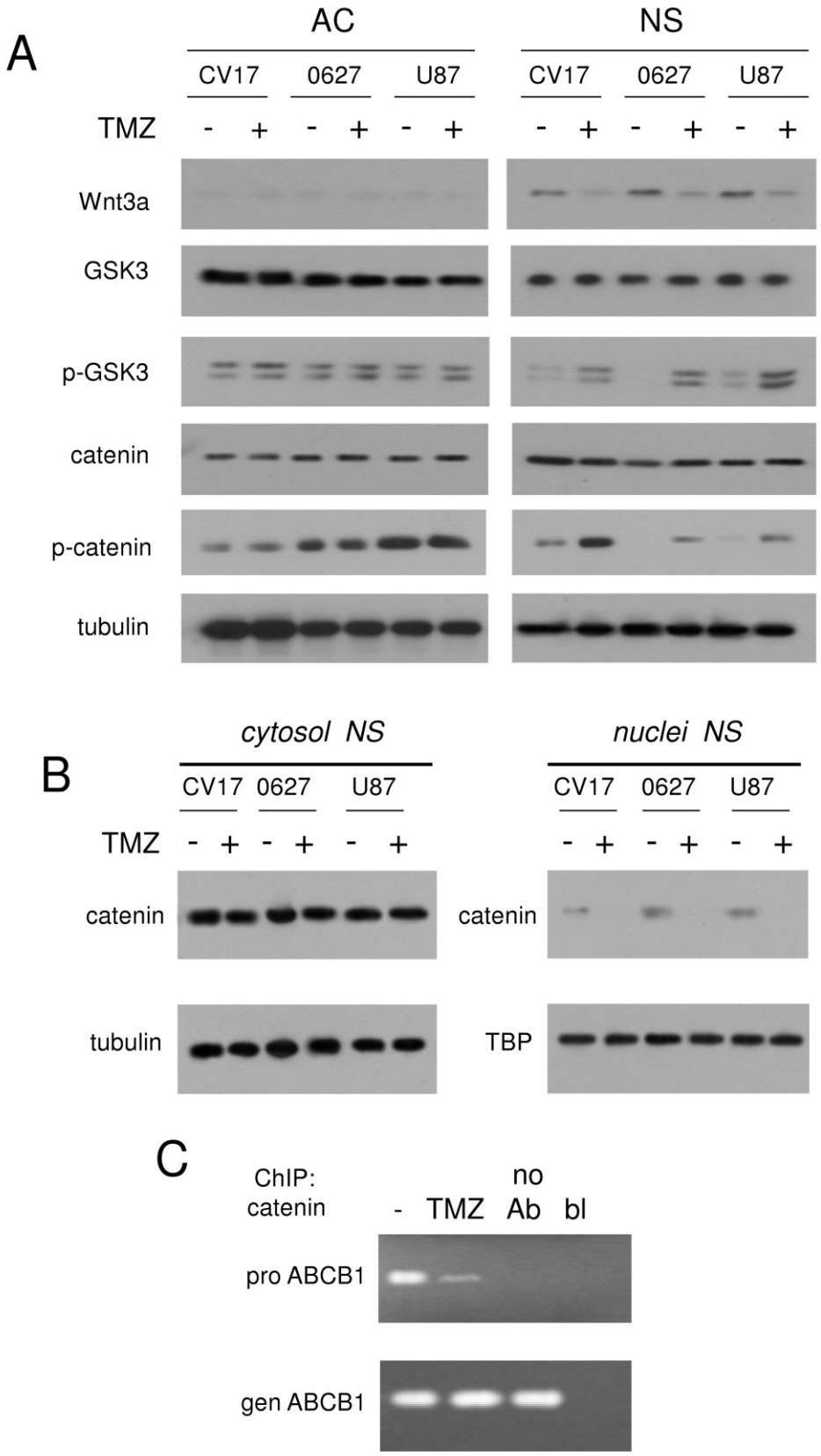
A
AC
NS
CV17
0627
U87
CV17
0627
U87
TMZ
- + - + - +
- + - + - +
Wnt3a
GSK3
p-GSK3
catenin
p-catenin
tubulin
B
cytosol NS
nuclei NS
CV17 0627 U87
CV17 0627 U87
TMZ
- + - + - +
- + - + - +
catenin
catenin
tubulin
TBP
C
ChIP:
catenin
no
- TMZ Ab bl
pro ABCB1
gen ABCB1

Figure 8

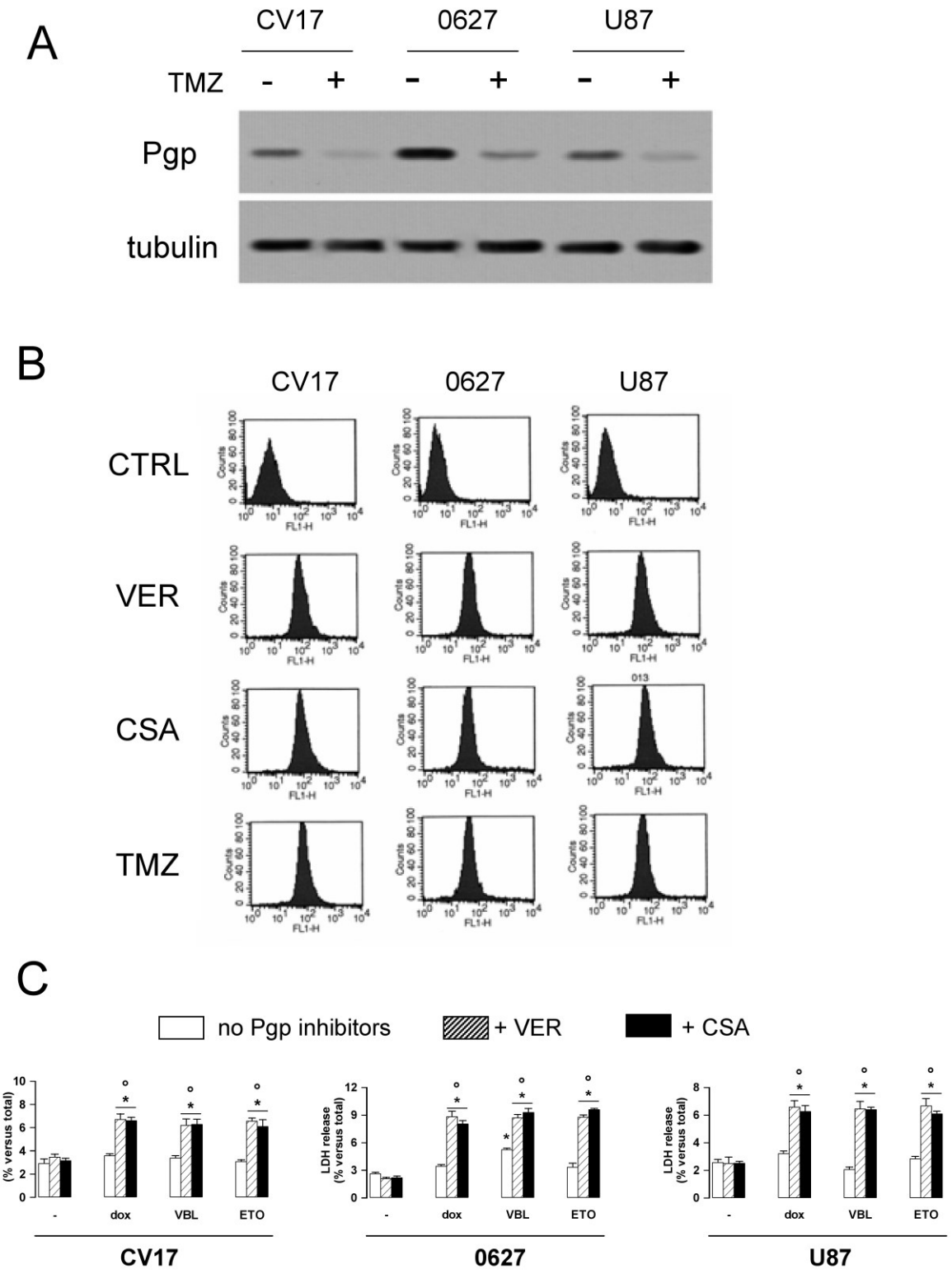
A
CV17
0627
U87
TMZ
-
+
-
+
-
+
Pgp
tubulin
B
CV17
0627
U87
CTRL
VER
CSA
TMZ
Counts
FL1-H
C
no Pgp inhibitors
+ VER
+ CSA
LDH release (% versus total)
-
dox
VBL
ETO
CV17
0627
U87

Supplementary Figure 1

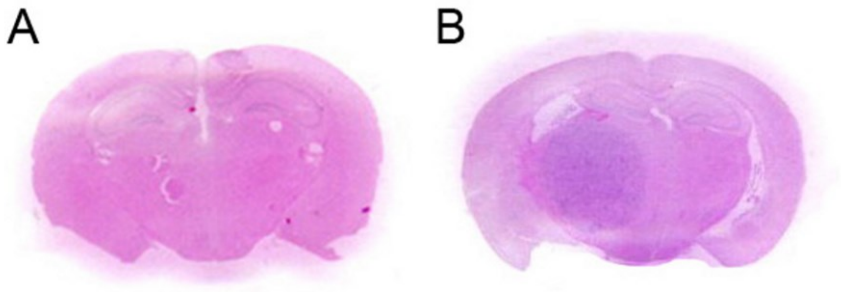

Supplementary Figure 2

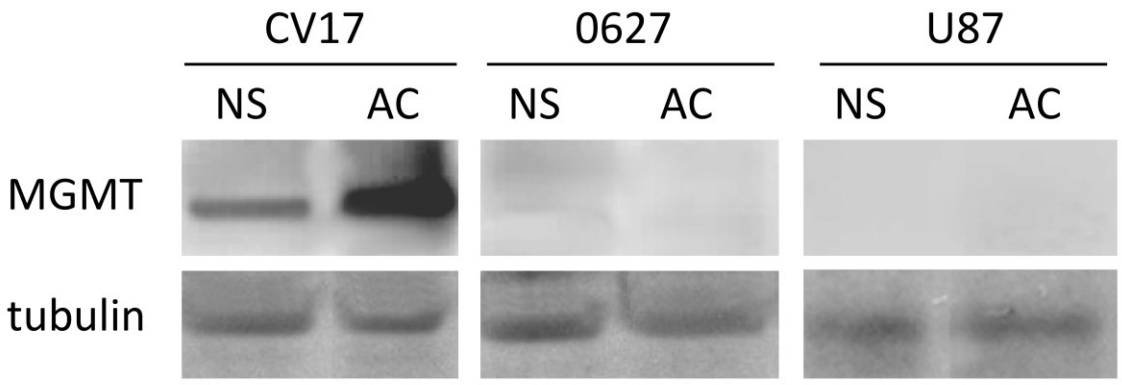

Supplementary Figure 3

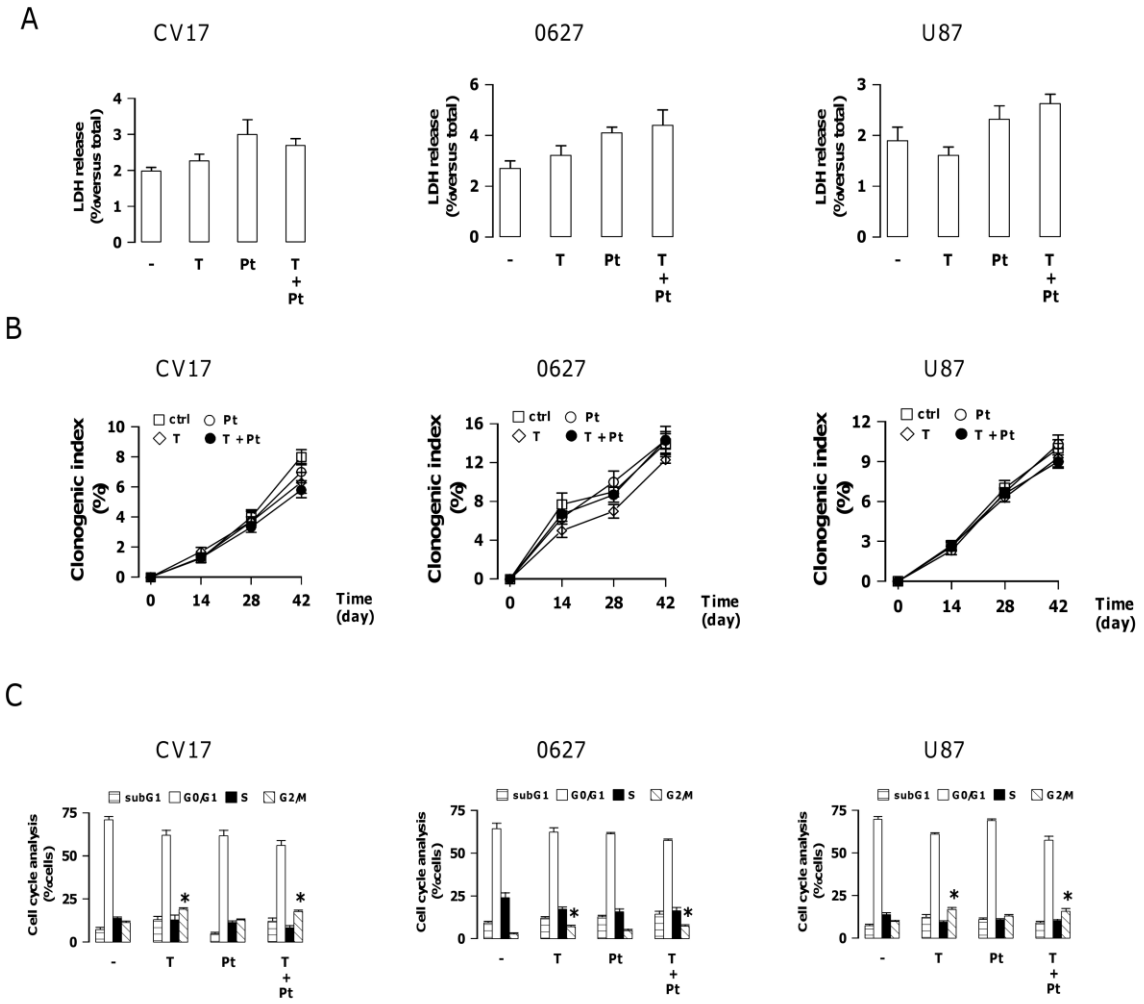

Supplementary Figure 4

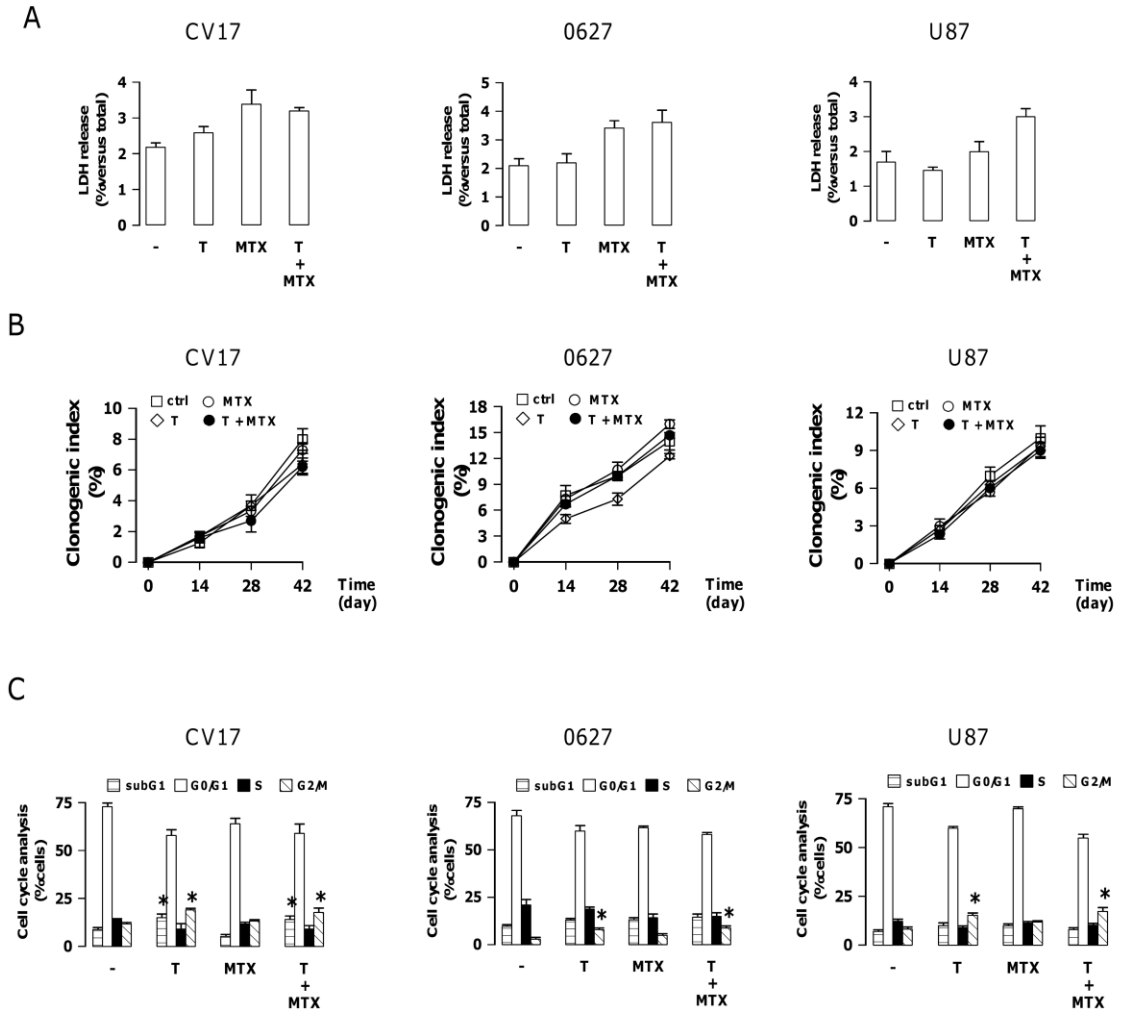

Supplementary Figure 5

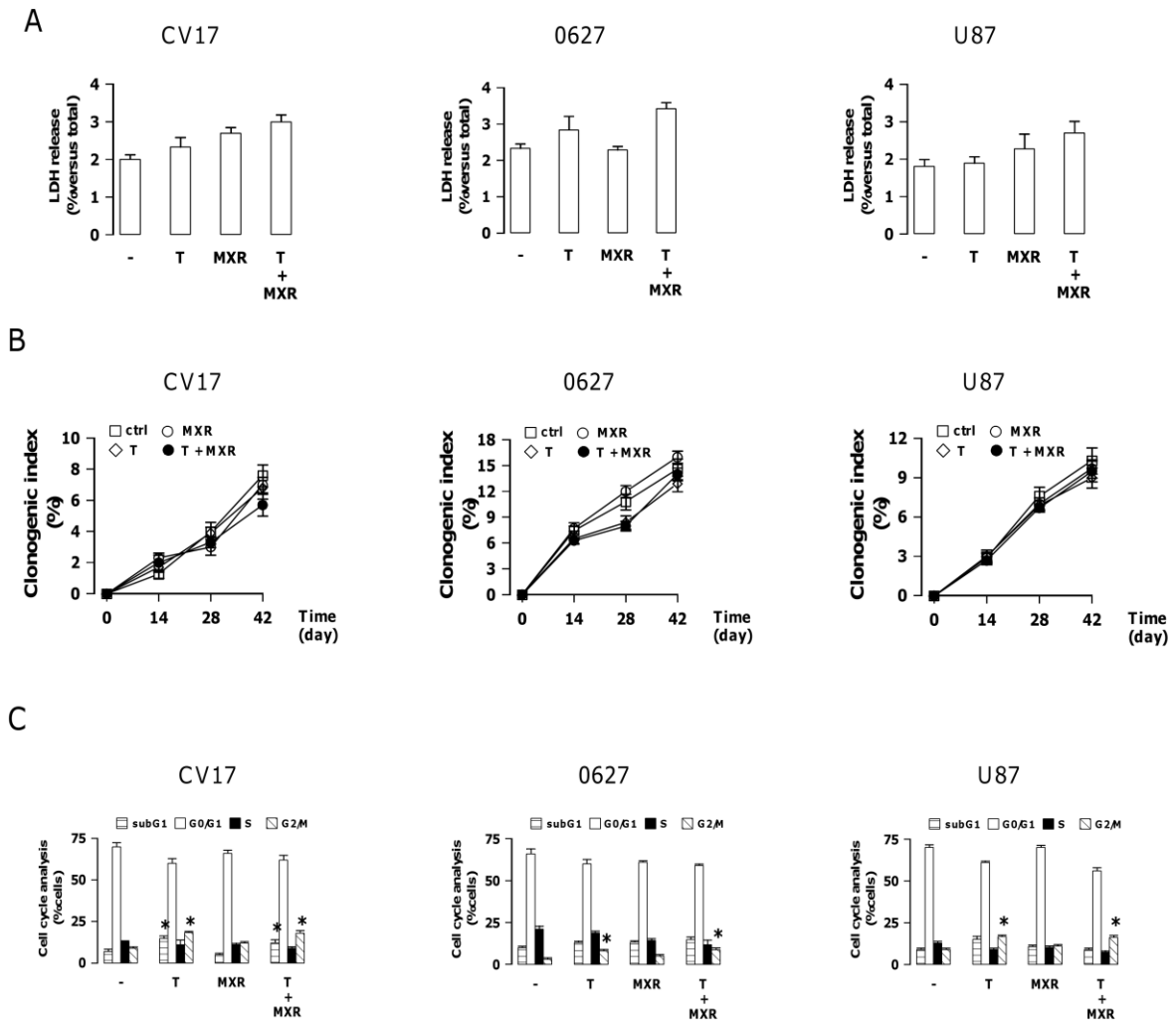

Supplementary Figure 6

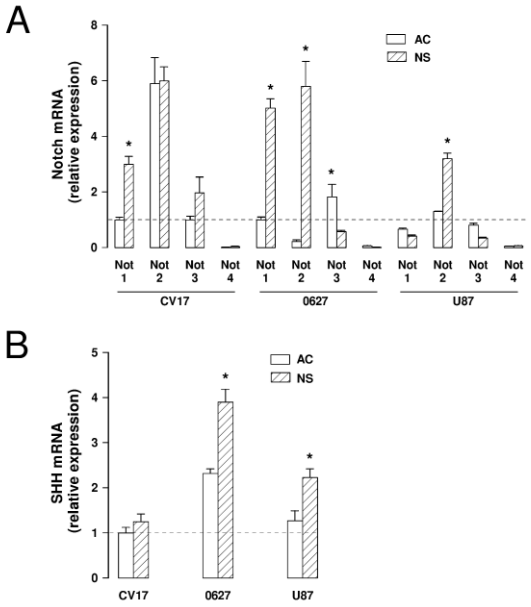

Supplementary Figure 7

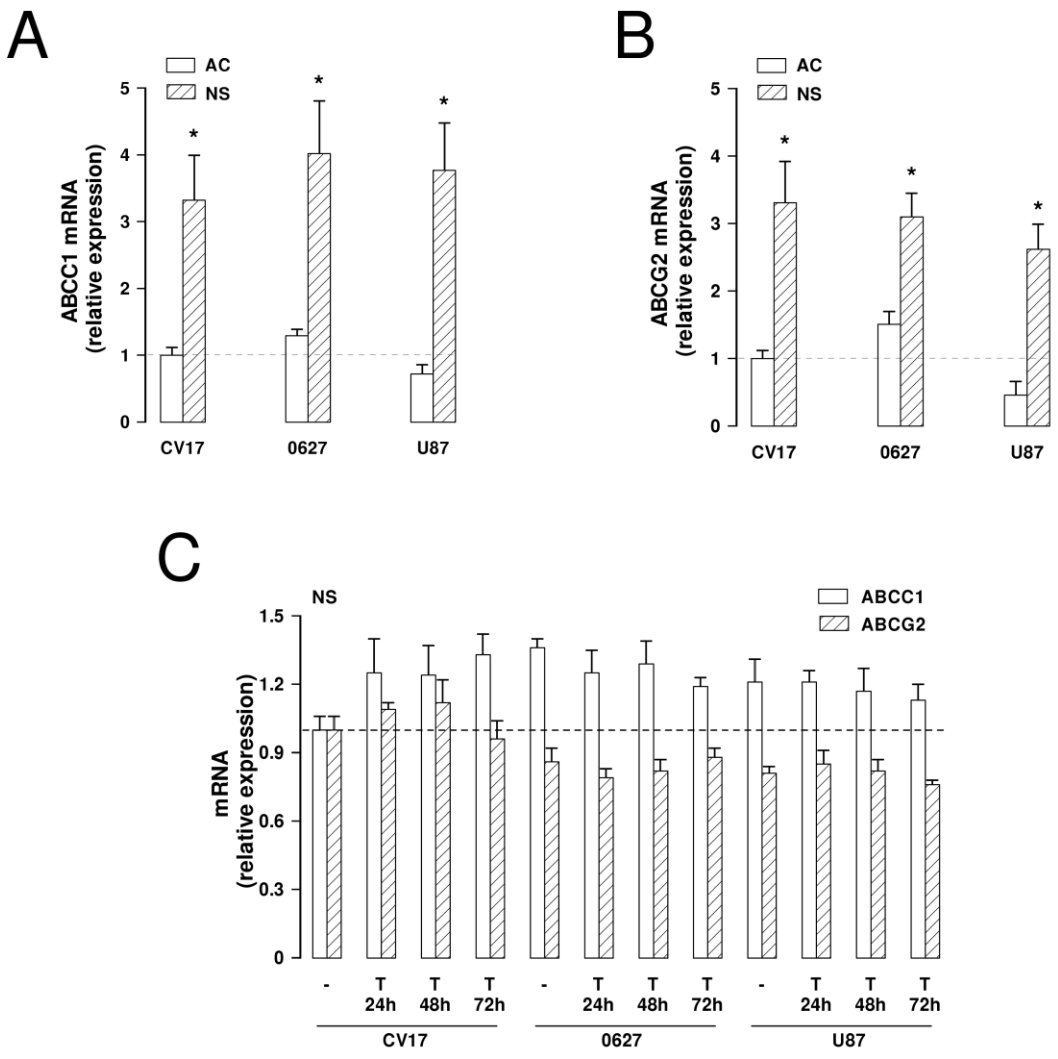

Supplementary Figure 8

A

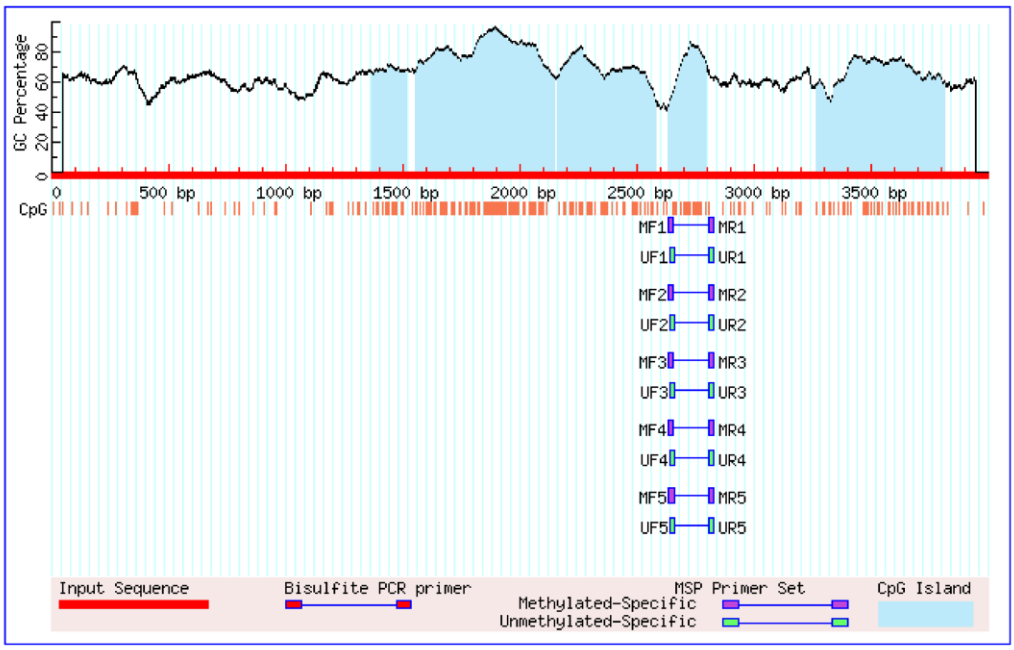

B

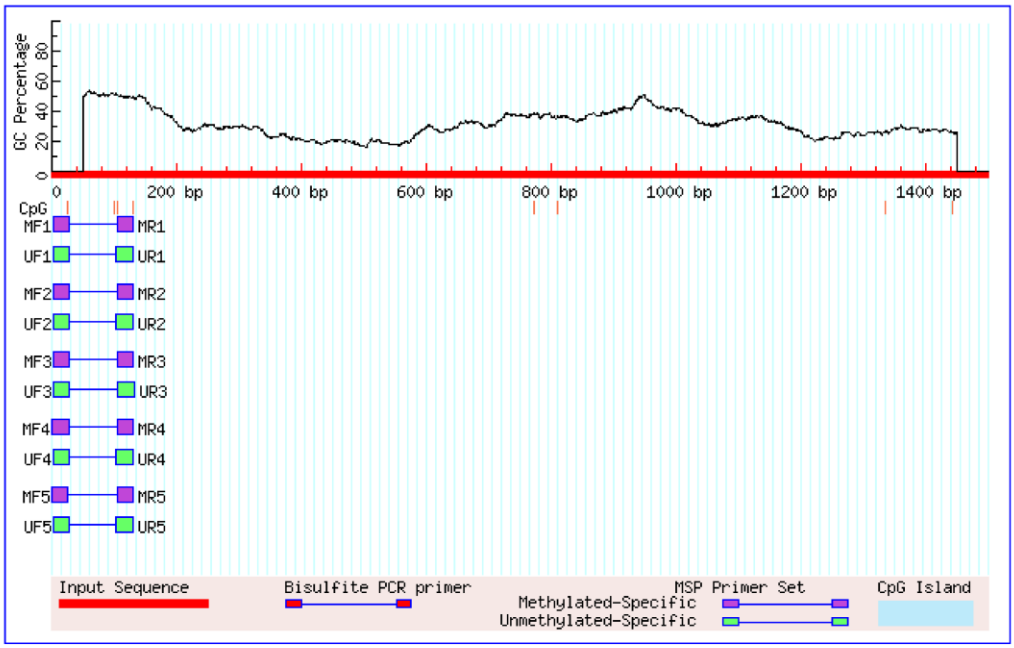

Supplementary Figure 9

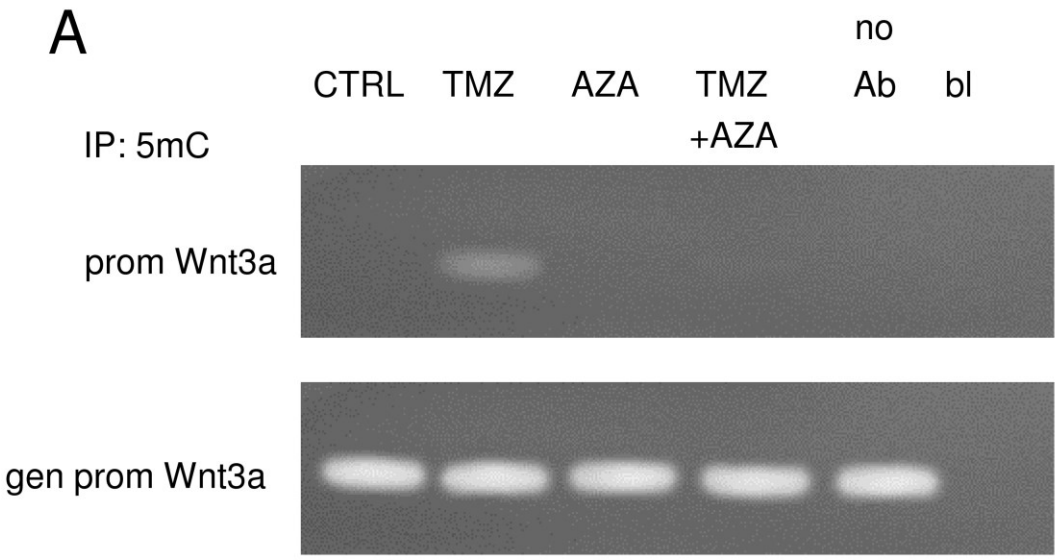

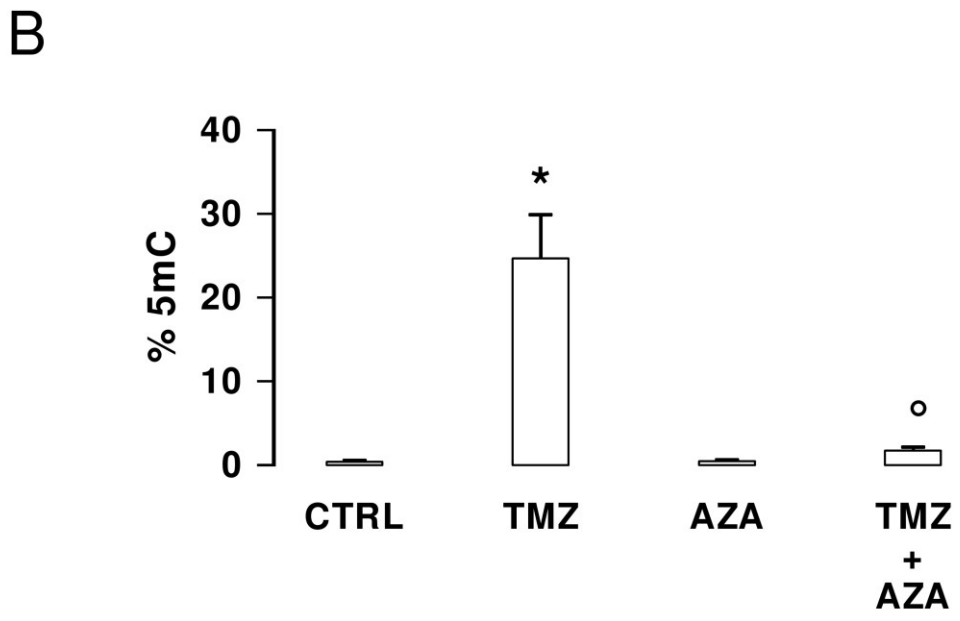

Supplementary Figure 10

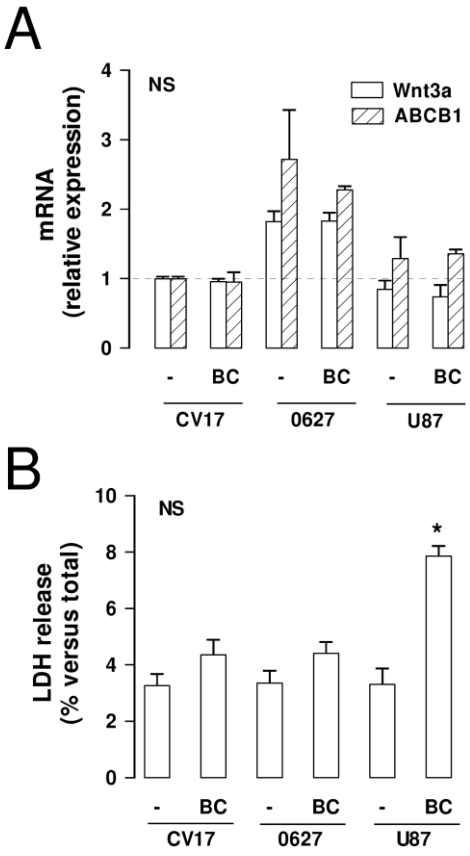

Supplementary Figure 11

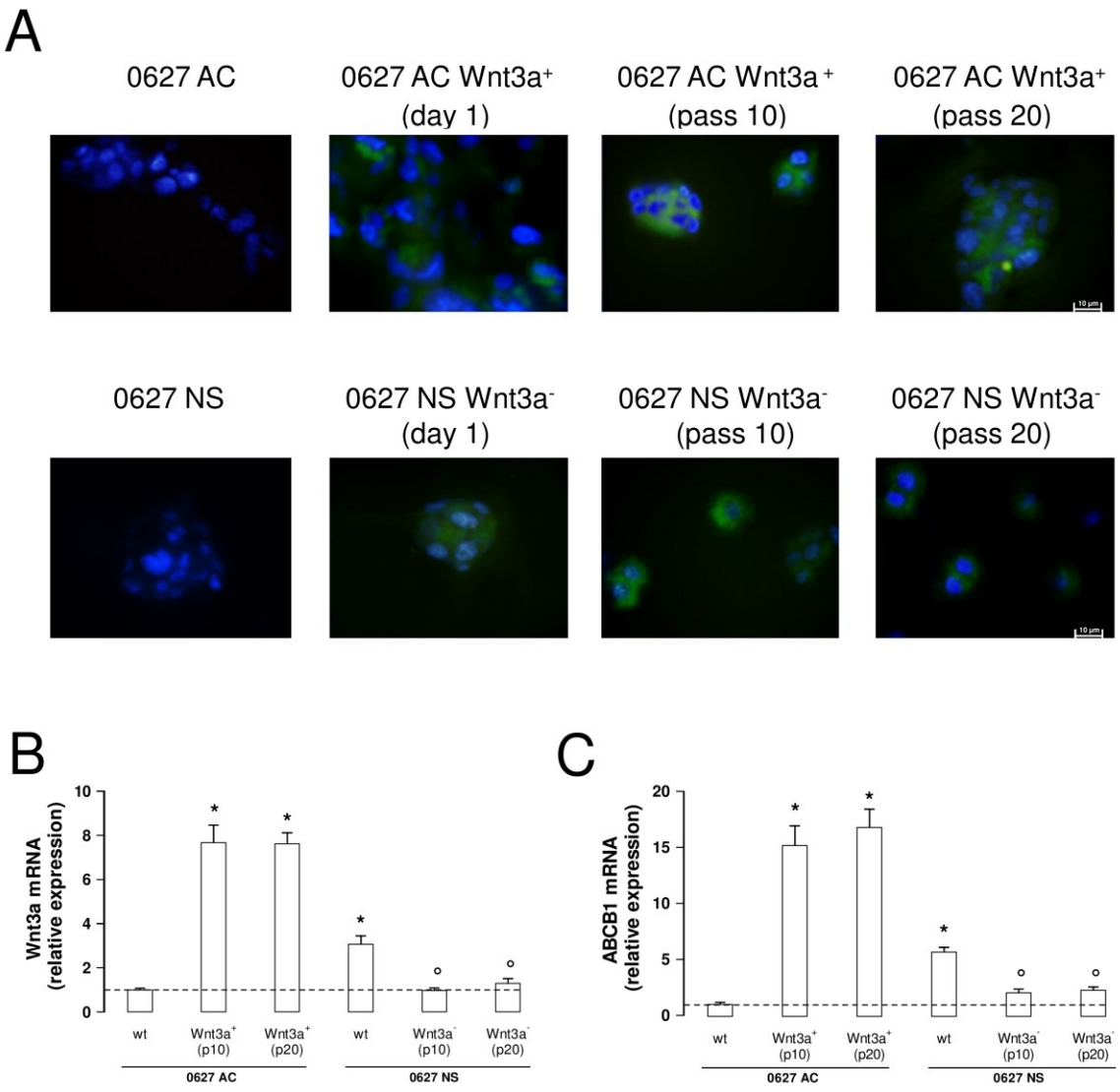

Supplementary Figure 12

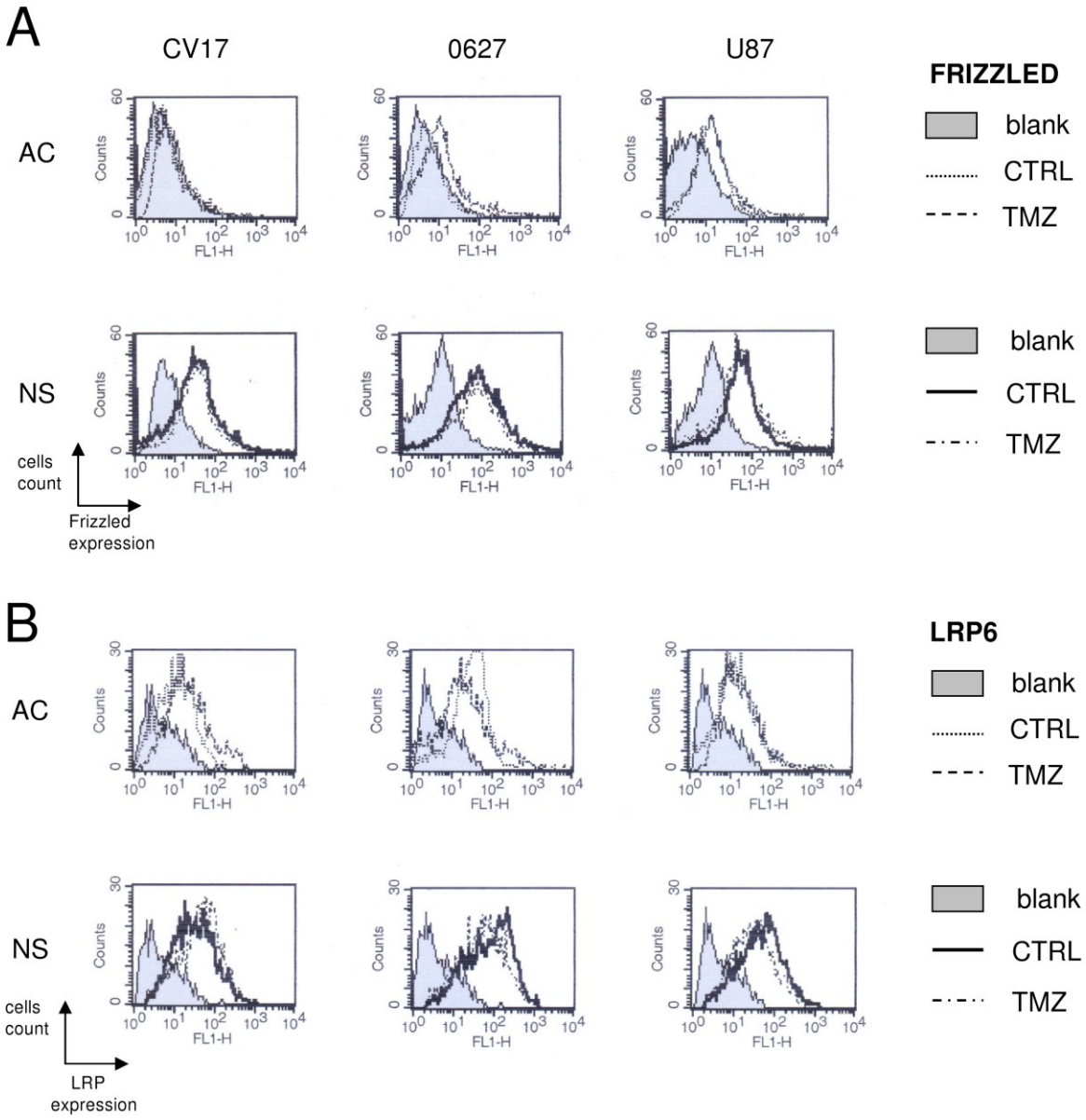

Supplementary Figure 13